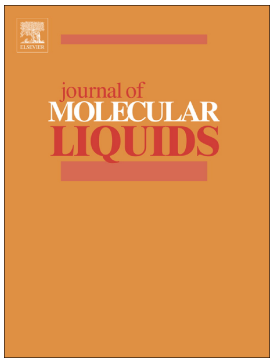

Physical properties and solid-liquid equilibria for hexafluorophosphate-based ionic liquid ternary mixtures and their corresponding subsystems

Anya F. Bouarab, Mónia A.R. Martins, Olga Stolarska, Marcin Smiglak, Jean-Philippe Harvey, João A.P. Coutinho, Christian Robelin

PII: S0167-7322(20)31762-1

DOI: https://doi.org/10.1016/j.molliq.2020.113742

Reference: MOLLIQ 113742

To appear in: *Journal of Molecular Liquids*

Received date: 23 March 2020

Revised date: 20 June 2020

Accepted date: 1 July 2020

Please cite this article as: A.F. Bouarab, M.A.R. Martins, O. Stolarska, et al., Physical properties and solid-liquid equilibria for hexafluorophosphate-based ionic liquid ternary mixtures and their corresponding subsystems, *Journal of Molecular Liquids* (2020), https://doi.org/10.1016/j.molliq.2020.113742

Physical Properties and Solid-Liquid Equilibria for Hexafluorophosphate-based Ionic Liquid Ternary Mixtures and their Corresponding Subsystems

Anya F. Bouarab[1], Mónia A. R. Martins[2], Olga Stolarska[3], Marcin Smiglak[4], Jean-Philippe Harvey[1], João A. P. Coutinho[2], and Christian Robelin[1,*]

[1] Centre for Research in Computational Thermochemistry (CRCT), Department of Chemical Engineering, Polytechnique Montréal, C.P. 6079, Succursale "Downtown", Montréal, Québec, H3C 3A7, Canada

[2] CICECO – Aveiro Institute of Materials, Department of Chemistry, University of Aveiro, 3810-193 Aveiro, Portugal

[3] Faculty of Chemistry, Adam Mickiewicz University, Poznań, Poland

[4] Poznan Science and Technology Park, Adam Mickiewicz University Foundation, Poznań, Poland

[*] Corresponding author (e-mail: christian.robelin@polymtl.ca)

Abstract :

Mixing ionic liquids is a simple and economical method of exploiting their tunability and allows to use ionic liquids with high melting temperatures for low-temperature applications through the formation of eutectic mixtures. In this study, the phase diagrams of the $[C_4mpy][PF_6]$-$[C_4mpip][PF_6]$-$[C_4mpyrr][PF_6]$ ternary system (where $[C_4mpyrr]$=1-butyl-1-methylpyrrolidinium; $[C_4mpy]$ = 1-butyl-3-methylpyridinium; $[C_4mpip]$=1-butyl-1-methyl-piperidinium) and all of its unary and binary subsystems were measured and modelled using the Modified Quasichemical Model and the Compound Energy Formalism for the liquid and relevant solid solutions, respectively. The phase diagram determination allowed for density and viscosity measurements over the entire composition range, from temperatures close to the liquidus up to about 110°C. In addition, the thermal and physical properties of the ionic liquid $[C_4mim][PF_6]$ ($[C_4mim]$=1-butyl-3-methylimidazolium) were measured. A new viscosity model was proposed to describe mixtures and was compared to the Grunberg-Nissan mixing law. The proposed model exhibited a better predictive ability for the viscosity data of ternary mixtures compared to the Grunberg-Nissan mixing law with the same number of adjustable parameters. The limits of the proposed viscosity model were analyzed in light of the Gibbs-Adam theory, using viscosity and configurational entropy data for $[C_4mim][PF_6]$.

1. Introduction

An ionic liquid is a salt generally composed of at least one bulky and asymmetric organic ion (most of the time the cation) that is liquid at a temperature lower than the consensual and arbitrary limit of 100°C. Increased intermolecular distances due to large ion size and charge delocalization in ions with resonance structures weaken the electrostatic interactions while the lack of symmetry and large conformational degrees of freedom in the liquid lead to large entropies of fusion. All those factors combined result in melting temperatures much lower than that of most inorganic salts. In addition to that property, their ionic nature confers them low vapour pressure, and thermal and chemical stability over a large temperature range. They were designated, due to their potential recyclability and their ability to dissolve a plethora of compounds, as "green solvents for the future" [1] with the ambition to replace conventional solvents in existing processes or to develop new technologies. However, some drawbacks to the extensive application of ionic liquids are their high synthesis cost and viscosity. Ionic liquids gained significant interest in the early 2000s when Seddon introduced them as designer solvents [2], with the possibility of fine-tuning their physicochemical properties to suit an application of interest. This has been achieved using different strategies: synthesis of new ions comprising specific functional groups known as Task-Specific Ionic Liquids (TSIL) [3], variation of cation-anion combinations with over 1 million of possibilities, or mixtures of ionic liquids [4]. The latter is an interesting alternative pathway to new ionic liquids since mixtures are easier, and often cheaper, to prepare. They also allow to explore more cation/anion combinations. For example, some ionic liquids with short alkyl chain are solid at room temperature but would feature better transport properties than their longer alkyl chain analogues due to the suppression of tail group aggregation and easier molecular reorientation [5]. The formation of eutectic mixtures, when considering the use of multicomponent materials, increases the liquid range and allows for their use in low-temperature applications. Mixtures of ionic liquids have been investigated for their use as electrolytes in capacitors [6, 7], supercapacitors [8, 9], Li-ion batteries [10-12] and dye-sensitized solar cells [13, 14] but also for bio-based polymer dissolution [15], CO_2 absorption [5, 16-18] and metal extraction [19].

Numerical simulations such as finite volume element methods are nowadays common tools to speed up the design of processes by virtually exploring the impact of different operating variables and reactor geometries on their thermo-physical behavior. To be accurate, these simulations require large databases and accurate models of self-consistent physicochemical properties. More specifically, the viscosity is a key property to evaluate when a liquid phase is involved in the modelled process, as it affects performance in terms of mass and charge transport. Models based on Free Volume Theory [20, 21], Hard-sphere theory [22], Eyring activated-state theory [23, 24] and the geometric similitude concept [25] have been proposed in the literature for modelling the viscosity of ionic liquid mixtures. Those approaches are generally based on the extension of a model for pure components through appropriate mixing rules. Good results are generally obtained except at low temperatures and/or high pressures where higher deviations between calculated and experimental values are observed. So far none of these approaches have been tested for eutectic mixtures of ionic liquids below the melting point of their corresponding pure components, nor were they extended to ternary mixtures, mostly because of the lack of corresponding data in the literature. Most experimental viscosity data reported for binary mixtures of ionic liquids were collected for room-temperature ionic liquids (RTIL) above the pure components' melting temperature. The viscosity of those mixtures was usually calculated with the Grunberg-Nissan [26] or the Katti-Chaudhri [27] mixing law and there is generally little deviation from the ideal mixing case [28]. To the best of our knowledge, only the recent viscosity data of three common-cation binary mixtures based on 1-butyl-3-methylimidazolium by Vieira *et al.* [29] and 1-ethyl-3-methylimidazolium by Yambou *et al.* [7] cover large temperature and composition ranges. In both cases, the viscosity of every binary mixture was fitted using the Vogel-Fulcher-Tamman [30-32] equation giving a set of parameters specific to each composition. Data for ternary ionic liquid mixtures are scarce in the literature and we are only aware of the measurements reported by Castiglione *et al.* [33] for the equimolar compositions of a ternary mixture based on the 1-butyl-1-methylpyrrolidinium cation and of its binary subsystems. The authors calculated the Arrhenius activation energy of viscous flow for the ternary mixture using activation energies from the pure components and Grunberg-Nissan parameters derived from binary data. A good agreement was obtained between the calculated and experimental values.

One of the challenging aspects of the viscosity modelling of ionic liquids is their departure from Arrhenian temperature-dependence, defined by Angell as their "fragility" [34]. There is to this date no generally accepted theory to account for this behavior. The viscosity of fragile liquids increases rapidly with temperature decrease. In the case of a eutectic mixture, a larger temperature range is considered, and the viscosity might increase significantly near the liquidus temperature. This would explain why some mixtures tend to undergo supercooling, and why in some cases the crystalline phase never forms on practical timescale.

While they are not, strictly speaking, ionic liquid mixtures, it is worth mentioning some viscosity models applied to the viscosity of Deep-Eutectic solvents (DES). In these, the focus is more often put on temperature ranges closer to the liquidus. Crespo *et al.* [35] applied the Free Volume theory coupled with the PC-SAFT equation of state [36] to the viscosity of three choline chloride-based DES over a large pressure range using an individual-component approach. The latter is opposed to a pseudo-pure approach in which the DES-by definition a mixture- is considered as a pure component and the derived model parameters are specific to the composition considered. The pseudo-pure approach, as used in [37], prevents the calculation of viscosity over a wide range of compositions. Mjalli and Naser [38] developed a model accounting for the temperature and composition dependence of nine choline chloride-based DES, without deriving pure component parameters. This limitation is primarily due to choline chloride decomposition prior to melting which makes it impossible to measure its liquid state viscosity. Most of the models cited above require the estimation of the density or compressibility factor Z, using an appropriate Equation-of-State (EoS). The results of the method therefore depend on the accuracy of the selected EoS. At atmospheric pressure, it has been shown that the super-Arrhenian behavior is primarily driven by an intrinsic effect of temperature rather than a density-driven change in free volume [39, 40]. Unless large pressure variations are considered, the viscosity of ionic liquids can thus be described without having to use density as a variable.

The main objective of this work is to measure and model the viscosity of the common-anion $[C_4mpyrr][PF_6]$-$[C_4mpy][PF_6]$-$[C_4mpip][PF_6]$ ($[C_4mpyrr]$ = 1-butyl-1-methylpyrrolidinium; $[C_4mpy]$ = 1-butyl-3-methylpyridinium; $[C_4mpip]$ = 1-butyl-1-methyl-piperidinium) ternary system and its binary and unary subsystems at atmospheric pressure over the largest composition and temperature ranges possible. Those ionic liquids are typically used in the preparation of

electrolytes in lithium-ion batteries [41, 42] and hybrid supercapacitors [43], thin-film membranes in microfabricated liquid junction reference electrodes [44], and carbon-composite electrodes [45].

These viscosity data are then used to assess and parametrize a viscosity model based on the MYEGA equation [46]. The prediction capability of the latter is finally tested on the ternary viscosity data and compared to that of the Grunberg-Nissan mixing law. The viscosity measurement for monophasic liquid samples requires knowledge of their liquidus temperature to ensure the experiment is not performed in a biphasic solid-liquid region. Because of that, the phase diagrams of the ternary system and its binary subsystems were determined experimentally and modelled using a CALPHAD-based approach. The CALPHAD (CALculation of PHAse Diagrams) method [47] is based on the sequential thermodynamic modelling of multi-component systems from a set of parameters used to describe lower-order subsystems [48]. More complex systems or systems not studied experimentally can be described using this method.

This work is the first step toward the development of a robust viscosity model for multicomponent ionic liquids over large composition and temperature ranges, and a follow-up on the development of thermodynamic models and databases for mixtures of ionic liquids [49, 50].

2. Materials and methods

2.1 Pure compounds

The pure compounds used in this work for the preparation of the binary and ternary mixtures were purchased from IoLiTec (Heilbronn, Germany). The IUPAC name, structure and abbreviation of the cations of the ionic liquids investigated in this work are shown in Figure 1 and their properties are listed in Table 1.

Prior to measurements, the pure compounds were dried at room temperature under high vacuum (10^{-5} Pa) for at least 48 hours. The water content was measured twice by Karl Fischer titration (Metrohm 831 Karl Fischer Coulometer) on pure dried compounds and the purity was confirmed by ^{1}H-NMR, ^{13}C-NMR, and ^{19}F-NMR spectroscopy. The water content was below 1000 ppm in

all cases (Table 1). Due to their high hygroscopicity, ionic liquids were stored and handled inside a dry-argon glove-box.

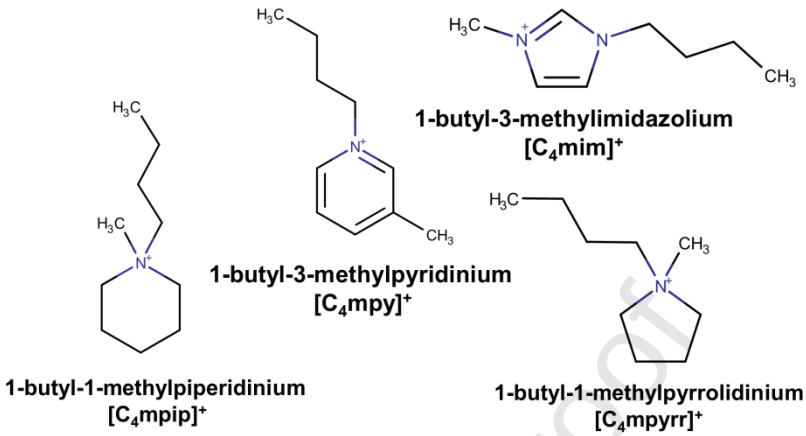

Figure 1: Structures and names of the cations of the studied ILs

Table 1: Properties of pure ionic liquids

	Molar mass (g/mol)	**Melting point* (°C)**	**Purity* (%)**	**Water content (ppm)**
[C_4mpy][PF_6]	295.21	52	99	43
[C_4mpip][PF_6]	301.26	81	99	395
[C_4mpyrr][PF_6]	287.23	87	99	511
[C_4mim][PF_6]	284.18	-8	99	393

*As reported by IoLiTec

2.2 Mixture preparation

Mixtures were prepared in a glove box under dry argon atmosphere and weighed accurately using an analytical balance model ALS 220-4N from Kern with an accuracy of ±0.002 g. Tightly closed vials with mixtures were heated under stirring until complete melting and then cooled at room temperature. The samples were stored in the glove-box or in a desiccator.

2.3 **Phase diagram determination**

Overall three different methods were used for the liquidus determination, depending on the nature of the sample.

DSC measurements were performed for all samples. Samples (2–5 mg) were hermetically sealed in aluminum pans inside the glovebox and then weighed using a micro analytical balance AD6 (PerkinElmer, USA, precision = 2×10^{-6} g). A Hitachi DSC7000X working at atmospheric pressure and coupled with a cooling system was used for the sample analysis. The equipment was previously calibrated with anthracene, benzoic acid, caffeine, decane, diphenylacetic acid, heptane, indium, lead, naphthalene, 4-nitrotoluene, potassium nitrate, tin, water and zinc, all with weight fraction purities higher than 99%. For each pure compound, at least 3 repeated cycles of (cooling-)heating-cooling were performed on at least 2 different samples. The transition temperatures and enthalpies were calculated using the average of all heating cycles (except the first one) for all samples studied. For mixtures, only one (cooling-)heating cycle was performed on a single sample. When necessary, several cycles were performed. The cooling and heating rates were respectively 5 K/min and 2 K/min. Each temperature was taken as the peak temperature upon heating.

In addition, the capillary method, as already described by [51],was used to determine the liquidus temperature of completely recrystallized samples and of pure compounds (solid at room temperature). Samples were mashed in the glove box into a powder that was then filled into a capillary. The melting points were determined with an automatic glass capillary device model M-565 from Bücchi, which has a temperature resolution of 1 K. The temperatures were taken as the average of triplicate measurements.

For other selected samples with a paste-like consistency, a visual method was also used. Mixtures were gradually heated in an oil bath until complete melting and the temperature was controlled with a Pt100 probe possessing a precision of ±0.1 K. The temperature at which the last crystal disappeared was taken as the liquidus temperature. This procedure was repeated at least twice with good reproducibility.

2.4 **Viscosity and density measurements**

Density and viscosity were simultaneously measured using the automated SVM3001 Anton Paar rotational Stabinger viscometer-densimeter. Measurements were performed only once on heating by steps of 5 K from the closest temperature to the liquidus possible up to the maximum limit of 363 K. Triplicates were performed for the composition closest to the eutectic to assess the dispersion of the data, especially at low temperatures. The viscosities investigated with the viscometer were in the range of 20-3000 mPa.s, which corresponds to a shear rate comprised in a 3-300 s^{-1} interval. The viscosity of samples with a melting temperature higher than 55°C was not measured with the viscometer due to a limitation of its injection setup.

The viscosity of the three pure compounds $[C_4mpip][PF_6]$, $[C_4mpyrr][PF_6]$, and $[C_4mpy][PF_6]$, and of three compositions in the binary system $[C_4mpip][PF_6]$-$[C_4mpyrr][PF_6]$ was measured with a Physica MCR 501 rotational rheometer in a DG26.7 concentric cylinder system (DIN 54453) and in the cone-plate measuring system (diameter 60 mm, angle 2°). The rheometer measurements were carried out at three shear rates (3 s^{-1}, 50 s^{-1}, and 300 s^{-1}) for the sample of $[C_4mpy][PF_6]$, and at one shear rate (50 s^{-1}) for all other samples.

The water content of the mixtures was determined after each viscosity measurement and was found to be below 1000 ppm for all samples.

2.5 **Modelling**

The calculated phase diagrams were obtained using the FactSage thermochemical software [52]. The methodology applied to obtain the thermodynamic model parameters is thoroughly described in reference [49] and will not be reported here in its entirety for the sake of concision. A theoretical description of the thermodynamic models considered for the approach can be found in the Theory section.

The parameters of the viscosity model were obtained by regression using a Levenberg-Marquardt algorithm as implemented in the "Optimization" module of the Scipy computing library [53].

3. Theory

3.1 Thermodynamic model

The Modified Quasichemical Model in the Quadruplet Approximation (MQMQA) [54] was used to model the liquid phase. The latter considers the non-random distribution of the different constituents of a solution and describes it as an ensemble of clusters of variable size (pairs, quadruplets...) whose formation is favoured by intermolecular interactions. In the case of an ionic liquid, the formalism in the quadruplet approximation considers both first-(cation-anion) and second-(cation-cation and anion-anion) nearest-neighbour interactions, simultaneously (Figure 2).

Cations and anions are constrained by their ionic nature and are distributed only on their respective sublattice: cationic and anionic. Quadruplets are constituted of two cations (2^{nd}-nearest-neighbours) and two anions (also 2^{nd}-nearest-neighbours) and mix randomly constrained by an elemental mass balance. The quadruplet composition at equilibrium minimizes the total Gibbs energy of the melt at given nPT conditions.

In the case of a common-ion system, each quadruplet reduces to a 2^{nd}-nearest- neighbour pair.

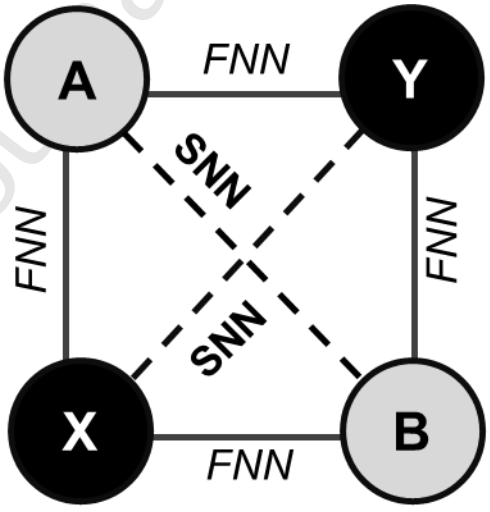

Figure 2: Schematic representation of a quadruplet (A and B are cations, and X and Y are anions. FNN = first-nearest-neighbour; SNN = second-nearest-neighbour)

The Gibbs energy of a common-anion binary melt AX-BX (abbreviated as A,B/X) is given by:

$$G = n_{AX} g^{o}_{AX} + n_{BX} g^{o}_{BX} - T\Delta S^{config} + \frac{n_{AB}}{2}\Delta g_{AB/X} \quad (1)$$

where n_{AX} and n_{BX} as well as g^{o}_{AX} and g^{o}_{BX} are the number of moles and molar Gibbs energies of the pure AX and BX components, respectively. ΔS^{config} is the configurational entropy of mixing given by randomly distributing the 2nd-nearest-neighbour cation-cation pairs. n_{AB} is the number of moles of (A-X-B) cation-cation pairs and $\Delta g_{AB/X}$ is the Gibbs energy change of the following pair-exchange reaction:

$$(A-X-A)_{pair} + (B-X-B)_{pair} = 2(A-X-B)_{pair};\ \Delta g_{AB/X} \quad (2)$$

$\Delta g_{AB/X}$ is expanded as an empirical polynomial in terms of the second-nearest-neighbour cation-cation pair fractions and the set of coefficients that permit to best reproduce the available phase diagram data is retained. For further details on the thermodynamic model used for the liquid phase, one is referred to [49] where all equations are given for the common-anion quaternary liquid [C_3mim][PF_6]-[C_3mpyrr][PF_6]-[C_3mpy][PF_6]-[C_3mpip][PF_6]. By analogy with the latter system previously modelled, for the [C_4mpyrr][PF_6]-[C_4mpy][PF_6]-[C_4mpip][PF_6] ternary liquid, all 2nd-nearest-neighbour coordination numbers were set to 6.0.

The solid solutions relevant for the present work are those for the binary system [C_4mpyrr][PF_6]-[C_4mpip][PF_6]. These were both modelled using the Compound Energy Formalism (CEF) [55]. The cations $[C_4mpip]^+$ and $[C_4mpyrr]^+$ reside on the cationic sublattice C while the anion $[PF_6]^-$ resides on the anionic sublattice A. The molar Gibbs energy of each solid solution is then given by the following equation:

$$\mathrm{G} = y^{C}_{[C_4mpip]^+} G^{o}_{[C_4mpip]^+:[PF_6]^-} + y^{C}_{[C_4mpyrr]^+} G^{o}_{[C_4mpyrr]^+:[PF_6]^-} + \mathrm{R}T\left(y^{C}_{[C_4mpip]^+} lny^{C}_{[C_4mpip]^+} + y^{C}_{[C_4mpyrr]^+} lny^{C}_{[C_4mpyrr]^+}\right) + \mathrm{G}^{\mathrm{E}} \quad (3)$$

In equation (3), $y^{C}_{[C_4mpip]^+}$ and $y^{C}_{[C_4mpyrr]^+}$ are the site fractions of each cation on the cationic sublattice C, and $G^{o}_{[C_4mpip]^+:[PF_6]^-}$ and $G^{o}_{[C_4mpyrr]^+:[PF_6]^-}$ are the standard molar Gibbs energies of the end-member components [C_4mpip][PF_6] (s_1,s_2) and [C_4mpyrr][PF_6] (s_2,s_3). G^E represents the molar excess Gibbs energy and is expressed as follows:

$$G^E = y^{C}_{[C_4mpip]^+} y^{C}_{[C_4mpyrr]^+} L_{[C_4mpip]^+,[C_4mpyrr]^+:[PF_6]^-} \quad (4)$$

The L factor may depend on the temperature and on the composition. In the latter case, Redlich-Kister terms as a function of site fractions are generally used.

3.2 **Viscosity Model**

The proposed model is based on the empirical equation proposed by Mauro *et al.* [46] and used to describe the viscosity of glass-forming liquids over large temperature ranges. This equation (see equation (9)) is derived from the Gibbs-Adam theory in which the relaxation time (or the viscosity) is related to the size of a cooperative rearranging region (CRR) [56]. The latter is defined as a region comprising a temperature-dependent number of particles (i.e. molecules or ions) *z*(T)* that can change its configuration independently of the surrounding particles.

$$\eta = \eta_\infty \exp\left(\frac{z^*(T)\Delta\mu}{RT}\right) \quad (5)$$

In equation (5), Δμ is the potential energy hindering the cooperative rearrangement per particle and η_∞ is a prefactor independent of temperature and representing the high-temperature limit of the viscosity.

The size of the CRR is found to be inversely proportional to the configurational entropy $S_c(T)$:

$$z^*(T) = \frac{N_A s_c^*}{S_c(T)} \quad (6)$$

where N_A is Avogadro's number and s_c* is the critical configurational entropy of the smallest possible cooperative region. Substitution of equation (6) into equation (5) gives:

$$\eta = \eta_\infty \exp\left(\frac{A}{TS_c(T)}\right) \quad (7)$$

where A is equal to $\frac{N_A s_c^* \Delta\mu}{R}$ and is considered as a fitting parameter.

The configurational entropy of the liquid as a function of temperature and composition is generally derived from heat capacity measurements. The practical limitation of the Gibbs-Adam model is the scarceness of calorimetric data in the literature for ionic liquids. We are only aware of the configurational entropy determination by Yamamuro *et al.* for [C_4mim]Cl [57] and by Ribeiro for [C_4mim][PF_6] [58].

To circumvent this issue, many mathematical expressions of the configurational entropy were proposed, most of them in order to provide a physical meaning to commonly used empirical expressions such as the Vogel-Fulcher-Tamman [30-32], the mathematically equivalent William-Landel-Ferry [59], and the Châtelier-Waterton [60, 61] equations.

Using the temperature-dependent constraint model applied to glass-forming liquids [62], Mauro *et al.*[46] proposed equation (8) which relates the configurational entropy to topological degrees of freedom.

$$S_c(T) = 3k_B N_A \ln\Omega \exp\left(-\frac{H}{RT}\right) \quad (8)$$

where k_B is the Boltzmann constant, N_A is Avogadro's number, Ω represents the number of degenerate configurations per degree of freedom and H is the activation enthalpy for breaking a constraint.

This leads to equation (9) which was originally proposed by le Châtelier [61] and Waterton [60].

$$\eta = \eta_\infty \exp\left(\frac{B(x)}{T}\exp\left(\frac{C(x)}{T}\right)\right) \quad (9)$$

$$B(x) = \frac{A}{3k_B N_A \ln\Omega} \text{ and } C(x) = \frac{H}{R}$$

Equation (9) is now referred to as MYEGA from the names of the authors of reference [46]. The parameters *B(x)* and *C(x)* are composition-dependent while η_∞ is a universal constant close to

$10^{-3.5}$ Pa.s and its value might vary with the nature of the liquid considered [63] . Consequently, the high-temperature limit of the viscosity η_∞ was set to that value.

MYEGA was preferred to the usually used Vogel-Fulcher-Tamman equation (10) since the description of viscosity over a large temperature range is generally better [63, 64] and it does not feature a singularity (i.e. divergence of viscosity or vanishing of configurational entropy) at finite temperature, which has to this date no physical justification.

$$\eta = \eta_\infty \exp\left(\frac{B}{T - T_0}\right) \tag{10}$$

B(x) and *C(x)* are proportional to potential energies and depend to some extent on the interactions between ions in the liquid. They are therefore estimated according to:

$$B(x) = \sum_j \sum_i \beta_{ij} x_{ij} \; ; \; C(x) = \sum_j \sum_i \gamma_{ij} x_{ij} \tag{11}$$

where x_{ij} represents the 2nd-nearest-neighbour cation-cation pair fraction given by the Modified Quasichemical Model in the pair approximation. The use of pair fractions instead of the product of mole fractions would allow for the description of mixtures with important short-range ordering. For a liquid solution close to ideality (i.e. $\Delta g_{AB/X} \rightarrow 0$) such as the $[C_4mpyrr][PF_6]$-$[C_4mpy][PF_6]$-$[C_4mpip][PF_6]$ ternary liquid investigated in the present work, it can be shown that $x_{ii} \rightarrow Y_i^2$ and $x_{ij} \rightarrow 2Y_iY_j$, where Y_i and Y_j are the "coordination-equivalent" fractions as defined in reference [49]. When all 2nd-nearest-neighbour coordination numbers are equal (as is the case in the present work), Y_i and Y_j reduce to the mole fractions x_i and x_j, respectively.

The parameters β_{ij} and γ_{ij} are estimated using the Lorentz-Berthelot mixing rule according to:

$$\beta_{ij} = (1 - k_{ij})\sqrt{B_i B_j} \; ; \gamma_{ij} = (1 - k_{ij})\sqrt{C_i C_j}$$
$$k_{ij} = \begin{cases} K, & for \quad i \neq j \\ 0, & for \quad i = j \end{cases} \tag{12}$$

where B_i and C_i (respectively B_j and C_j) are the two parameters in equation (9) required to best reproduce the available viscosity data for pure liquid i (respectively j).

K is an adjustable parameter. Note that k_{ij} is the same parameter in both expressions of *B(x)* and *C(x)*, thus leading to only one adjustable parameter (K) per binary mixture.

4. Results and discussion

4.1 Thermal behavior and phase diagram

4.1.1 Pure ionic liquids

The thermal events (temperatures and enthalpies) measured by DSC in this work for the pure compounds are reported in Table 2. For the sake of consistency, only the transition temperatures obtained by DSC were used in the thermodynamic model. A detailed description of the thermal behavior of $[C_4mim][PF_6]$ is available in the *Supporting Information*.

Table 2: Fusion and solid-solid transition properties of pure compounds

Compound	Transition	Enthalpy (kJ/mol)	Temperature (°C)
$[C_4mpy][PF_6]$	$S_1 \rightarrow S_2$	6 ± 1	41.6 ± 0.4
	$S_2 \rightarrow L$	15.7 ± 0.3	49.2 ± 0.7
$[C_4mpyrr][PF_6]$	$S_1 \rightarrow S_2$	2.18 ± 0.01	11.7 ± 0.2
	$S_2 \rightarrow S_3$	1.73 ± 0.01	42.2 ± 0.3
	$S_3 \rightarrow L$	5.5 ± 0.6	83.5 ± 0.2
$[C_4mpip][PF_6]$	$S_1 \rightarrow S_2$	4.6 ± 0.1	49.7 ± 0.3
	$S_2 \rightarrow L$	4.36 ± 0.02	79.8 ± 0.3

The C_3 analogues (i.e. in which the butyl group is replaced by a propyl group) of these compounds were studied by [65] and [66]. One is referred to [49] and [67] for a review of their fusion and solid-solid transition properties. While no solid-solid transitions were reported in the case of the $[C_3mpy][PF_6]$ and $[C_3mim][PF_6]$ ionic liquids, the C_4 analogues present a more complex thermodynamic behavior. Adding one $-CH_2-$ group to the alkyl chain results in increased flexibility and number of conformers for the cation.

In the case of $[C_4mpy][PF_6]$ (Figure 3a), there is substantial supercooling. Upon cooling, a large exothermic peak is followed by a smaller one of variable area, depending on the sample and the

cycle. Similar behaviour is encountered upon heating: a small endothermic peak is followed by a sharp and intense one. While the last peak is always present, independently of the cycle or of the sample, it is not the case for the small peak found around 42°C. We can thus assume that the last peak at around 49°C corresponds to the fusion of $[C_4mpy][PF_6]$ while the other one could be associated with a transformation from a polymorph that forms upon cooling to the most thermodynamically stable one. To the best of our knowledge, no prior DSC study was reported for $[C_4mpy][PF_6]$ to confront our results.

Both $[C_4mpip][PF_6]$ and $[C_4mpyrr][PF_6]$ present little supercooling (Figures 3b and 3c) with only a few degrees (1-5°C) between the peaks obtained upon cooling and heating. Indeed, we observed that those compounds crystallise quite rapidly. Contrary to what would have been predicted from the analogy with $[C_3mpip][PF_6]$, $[C_4mpip][PF_6]$ presents two allotropes instead of three. $[C_4mpyrr][PF_6]$ (Figure 3c) presents two endothermic solid-solid transitions upon heating: the first one is subsequent to the cold crystallisation from the supercooled liquid and is not observed upon cooling. The second one is observed at around 42°C and is reversible.

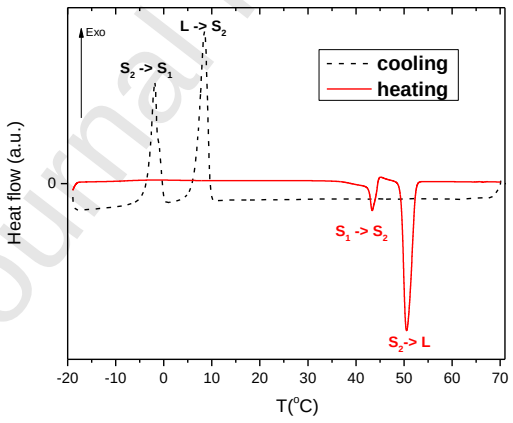

(a)

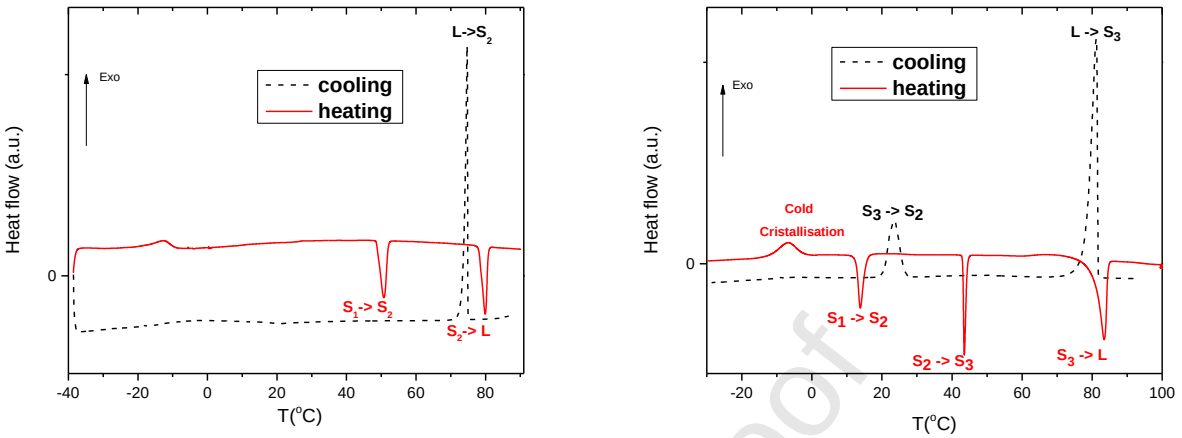

(b) (c)

Figure 3: Thermograms of: (a) [C_4mpy][PF_6]; (b) [C_4mpip][PF_6] and (c) [C_4mpyrr][PF_6]

The phase behaviour of [C_4mpyrr][PF_6] was already reported by Golding *et al.* [66], and our results agree within 5°C except for our melting temperature which is more than 10°C higher. It must be noted that the authors of the previously mentioned publication [66] synthesized the ionic liquid in their laboratory and no water content was reported although it was mentioned that the obtained solid was dried. At the time of publication, the effect of water content on the physical properties of ionic liquids was not fully recognized or assessed. It is possible that the presence of water decreased the observed melting temperature, explaining the discrepancy between the two experimental values. Since both DSC profiles are very similar, and the NMR peaks reported for [C_4mpyrr][PF_6] in [66] match the ones obtained in the present work, the possibility of different isomers or polymorphs can be ruled out.

4.1.2 Binary and ternary mixtures

4.1.2.1 Binary phase diagram with complete solid solution

In the binary system [C_4mpip][PF_6]-[C_4mpyrr][PF_6] (Figure 4a), the measured limiting slopes (represented as thin red lines) of the [C_4mpip][PF_6] and [C_4mpyrr][PF_6] liquidus curves substantially disagree with equation (13), which assumes no solid solubility:

$$\left(\frac{dT}{dx_m^{liquidus}}\right) = \frac{RT^2_{fusion(m)}}{\Delta h°_{fusion(m)}} \qquad at\ x_m = 1 \tag{13}$$

where R is the gas constant and $T_{fusion(m)}$ and $\Delta h°_{fusion(m)}$ are, respectively, the temperature of fusion and the molar enthalpy of fusion of the pure salt *m*. Therefore, two extensive solid solutions were introduced: one at high temperatures (HT-ss) between [C_4mpip][PF_6] (s_2) and [C_4mpyrr][PF_6] (s_3), and one at low temperatures (LT-ss) between [C_4mpip][PF_6] (s_1) and [C_4mpyrr][PF_6] (s_2).

Similar behaviour was already proposed by [65], [67] and [49] in the case of the C_3 analogues, where the only difference is the absence of an intermediate-temperature solid solution since [C_4mpip][PF_6] presents only two allotropes. While to the best of our knowledge no crystallographic data were reported for either [C_4mpip][PF_6] or [C_4mpyrr][PF_6], one can assume that, for the two solid solutions, the corresponding allotropes have the same crystal structure due to the similar structure of the cations. For the same reason, the binary liquid was assumed to be ideal. That is:

$$\Delta g_{[C_4mpip][C_4mpyrr]/[PF_6]} = 0 \tag{14}$$

The two solid solutions were described with the Compound Energy Formalism (CEF). The optimized excess Gibbs energy G^E of each solid solution is given in Table 3.

Table 3: Optimized excess Gibbs energies of the solid solutions in the [C_4mpip][PF_6]-[C_4mpyrr][PF_6] binary system

Solid solution	**Optimized G^E (J/mol)**
HT-ss	$275.0\ y^C_{[C_4mpyrr]^+} \times y^C_{[C_4mpip]^+}$
LT-ss	$y^C_{[C_4mpyrr]^+} \times y^C_{[C_4mpip]^+} \times \left[475.0 + 375.0\left(y^C_{[C_4mpyrr]^+} - y^C_{[C_4mpip]^+}\right)\right]$

4.1.2.2 Binary phase diagrams with a simple eutectic behavior

For both of the $[C_4mpip][PF_6]$-$[C_4mpy][PF_6]$ and $[C_4mpy][PF_6]$-$[C_4mpyrr][PF_6]$ binary systems (Figures 4b and 4c), a simple eutectic system with negligible solid solubility was assumed.

The optimized Gibbs energy of the quasichemical reaction (2) for each binary liquid is given in Table 4.

Table 4: Optimized Gibbs energy of reaction (2) for the eutectic-type phase diagrams

Binary system	**Optimized $\Delta g_{AB/[PF6]}$ (J/mol)**
$[C_4mpip][PF_6]$-$[C_4mpy][PF_6]$	275.0
$[C_4mpy][PF_6]$-$[C_4mpyrr][PF_6]$	732.2

One should note that the binary system $[C_4mpip][PF_6]$-$[C_4mim][PF_6]$ was investigated by DSC but thermal arrests were quasi-inexistant and several repeated cycles were necessary to hardly observe a peak. The data obtained were therefore not conclusive enough to perform a thermodynamic optimization. This may be due to the complex thermal behaviour of $[C_4mim][PF_6]$, preventing crystallisation of the binary mixtures from the supercooled liquid.

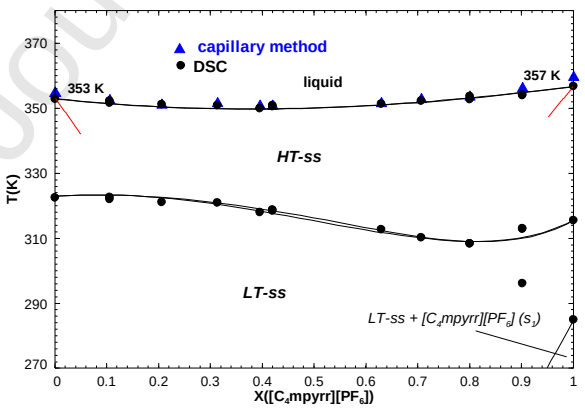

(a)

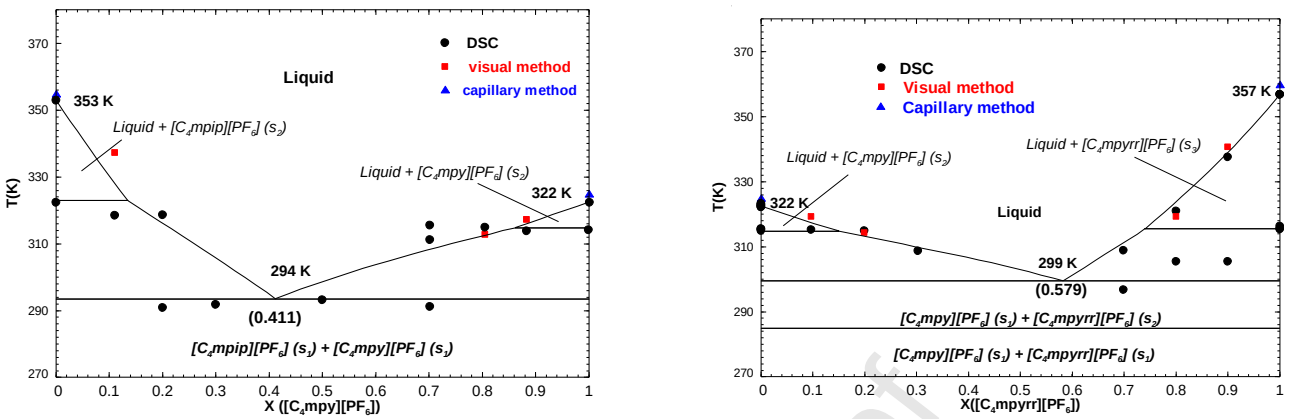

(b) (c)

Figure 4: Calculated phase diagrams of binary systems: (a) $[C_4mpip][PF_6]$-$[C_4mpyrr][PF_6]$ (The red lines represent the limiting slopes calculated with equation (13)); (b) $[C_4mpip][PF_6]$-$[C_4mpy][PF_6]$; (c) $[C_4mpy][PF_6]$-$[C_4mpyrr][PF_6]$

4.1.2.3 Ternary phase diagram $[C_4mpyrr][PF_6]$-$[C_4mpy][PF_6]$-$[C_4mpip][PF_6]$

For the ternary system, two isoplethal sections were investigated using DSC: one at constant 40 mol % $[C_4mpy][PF_6]$ and the other at a constant molar ratio $[C_4mpyrr][PF_6]/([C_4mpyrr][PF_6] + [C_4mpip][PF_6])$ of 0.60. The thermodynamic properties of the ternary liquid were calculated from the optimized model parameters for the three binary subsystems using a Kohler-Toop-like (asymmetric) interpolation method [68] with $[C_4mpy][PF_6]$ as the asymmetric component. This interpolation method was defined in reference [49]. Since all three optimized Gibbs energies of reaction (2) are constant, a Kohler-like (symmetric) interpolation method would give identical results. No ternary excess parameter was introduced for the liquid. The calculated liquidus projection of the $[C_4mpyrr][PF_6]$-$[C_4mpy][PF_6]$-$[C_4mpip][PF_6]$ system is shown in Figure 5 while the two calculated ternary isoplethal sections are displayed in Figure 6. As seen in the latter figure, agreement between the predicted phase diagram and the experimental data is satisfactory, keeping in mind that the optimized binary model parameters were not adjusted to better reproduce the ternary data. As shown in Figure 5, the minimum liquidus temperature corresponds to the binary eutectic reaction liquid = $[C_4mpy][PF_6](s_1)$ + $[C_4mpip][PF_6](s_1)$ at 294 K.

Thermal arrests below 273 K that were not predicted by the thermodynamic model were present in the isoplethal section at constant 40 mol % [C_4mpy][PF_6] (Figure 6b) and could not be interpreted. An in-depth analysis of those peaks would require information from coupled structural studies (optical microscopy, XRD, Raman, and NMR spectroscopy). The presence of metastable phase equilibria is suspected. This would be reasonable considering, as mentioned earlier, the known tendency of ionic liquids to polymorphism. Moreover, this phenomenon was also observed in the same ternary isoplethal section of the C_3 analogues (at constant 40 mol% of [C_3mpy][PF_6]) studied by [49].

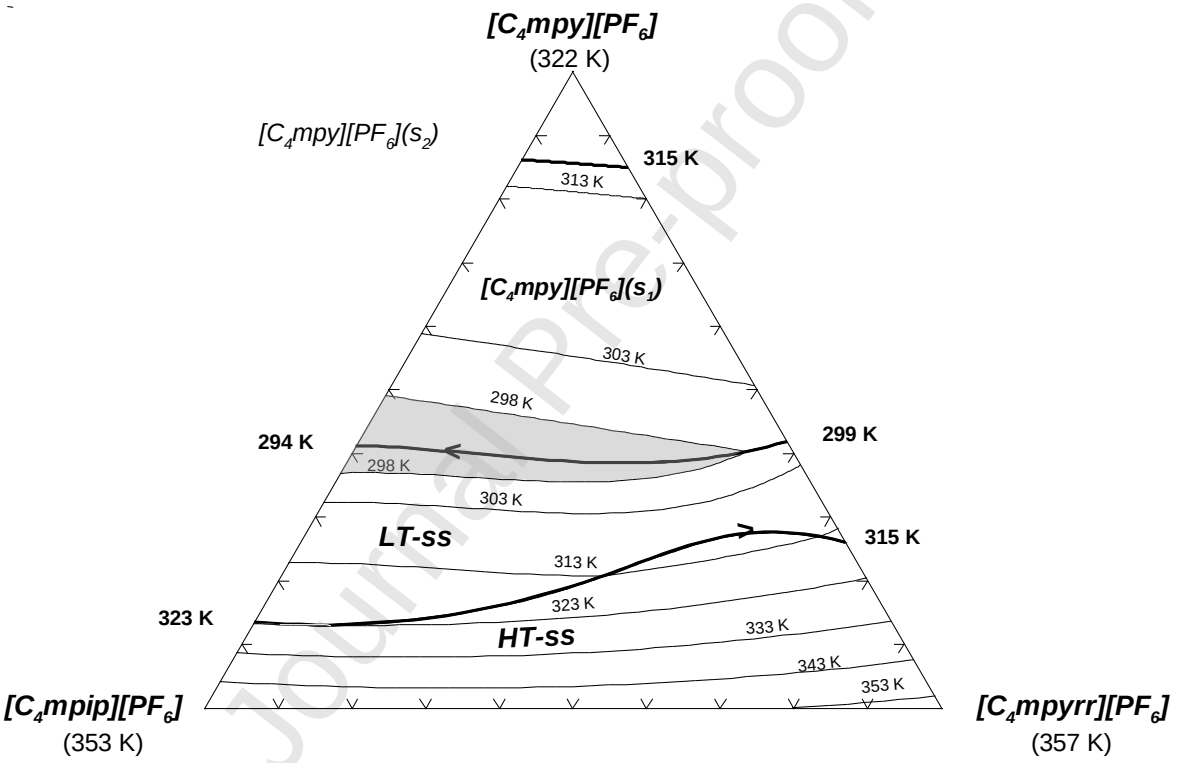

Figure 5: Calculated liquidus projection of the [C_4mpy][PF_6]-[C_4mpip][PF_6]-[C_4mpyrr][PF_6] system. The region of composition corresponding to room-temperature ionic liquid (RTIL) mixtures is highlighted.

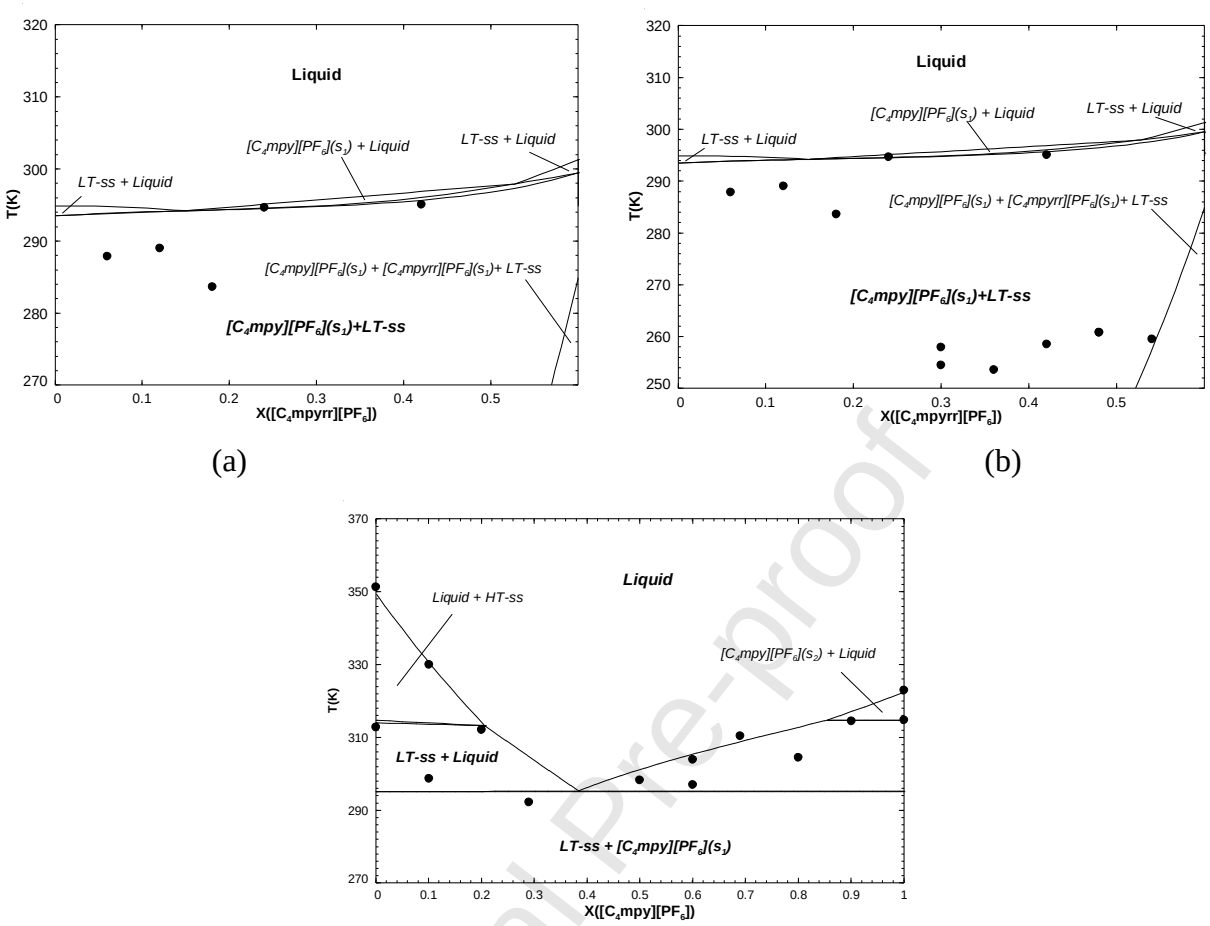

Figure 6: Calculated (predicted) ternary isoplethal sections in the $[C_4mpyrr][PF_6]$-$[C_4mpy][PF_6]$-$[C_4mpip][PF_6]$ system: (a) at 40 mol % $[C_4mpy][PF_6]$ from T = 270 to 320 K; (b) at 40 mol % $[C_4mpy][PF_6]$ from T = 250 to 320 K with intense thermal arrests below 273 K; (c) at a constant molar ratio $[C_4mpyrr][PF_6]$ / ($[C_4mpyrr][PF_6]$ + $[C_4mpip][PF_6]$) of 0.60.

4.2 **Density and Viscosity**

The density and viscosity of pure compounds, and their binary and ternary mixtures were measured by steps of 5 K from the closest possible temperature to the liquidus temperature of each composition up to the maximum limit of 363 K. Exceptions are $[C_4mpyrr][PF_6]$ and $[C_4mpip][PF_6]$ due to their high melting temperatures (> 353 K) and the corresponding binary mixtures due to the high liquidus temperature (> 343 K) over the entire composition range. In these cases, only the viscosity was measured using a rheometer up to 383 K. All data are given in the *Supporting Information*.

4.2.1 *Density*

The density of all liquid mixtures is linearly dependent on the composition (at a fixed temperature) and on the temperature (at a given composition). In general, the density decreases with the addition of either [C_4mpip][PF_6] or [C_4mpyrr][PF_6] and seems to display no significant deviation from ideal mixing. For the ternary mixtures with constant 40 mol % [C_4mpy][PF_6] at given temperature, the density only slightly increases as the [C_4mpyrr][PF_6] content increases, which suggests that [C_4mpip][PF_6] and [C_4mpyrr][PF_6] have close densities as expected by the similarities of their cations. All density measurements are available in the *Supporting Information.* As an example, the densities of the [C_4mpip][PF_6]-[C_4mpy][PF_6] binary mixtures investigated are displayed in Figure S2 in the *Supporting Information*.

4.2.2 *Viscosity*

4.2.2.1 *Pure ILs*

The compatibility between the Stabinger viscometer and the rheometer was confirmed by the comparison of both data sets obtained for [C_4mpy][PF_6] (Figure 7a). Moreover, the latter was found to be Newtonian (Figure 7b) for shear rates up to 300 s^{-1} over the entire temperature range studied (328.15-383.15 K).

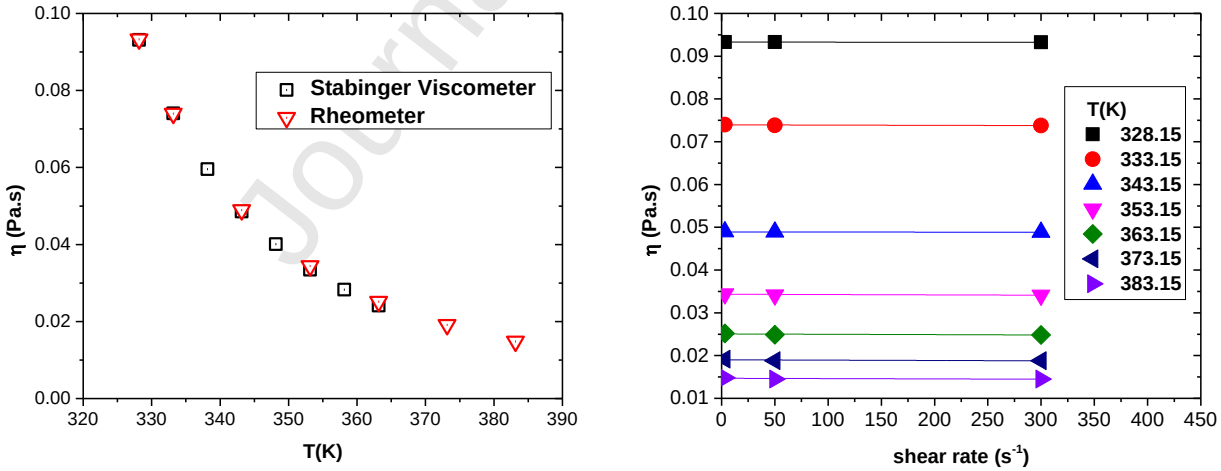

(a) (b)

Figure 7: (a) Comparison between the viscometer and rheometer measurements of the viscosity of [C_4mpy][PF_6]; (b) Newtonian behavior of [C_4mpy][PF_6] over large ranges of temperature and shear rate: lines are a guide for the eye.

The viscosity of the various pure ionic liquids investigated is shown in Figure 8a along with the corresponding Arrhenius plots (Figure 8b). The aromatic ionic liquids have a lower viscosity than the non-aromatic ones. This could be explained in part by the delocalization of the positive charge due to the cation aromaticity, thus diminishing the strength of electrostatic interactions. This trend was already observed for similar cations with the bis(trifluoromethyl sulfonyl)imide ($[NTf_2]^-$) anion [69].

Ionic liquids are generally fragile liquids [70-72] and usually, their viscosity cannot be represented with an Arrhenius-type equation:

$$\eta = A \exp\left(\frac{B}{T}\right) \tag{15}$$

We followed the common practice of assessing the deviation from Arrhenian behavior by performing linear fits to the logarithm of the viscosity as a function of the reciprocal of temperature (Figure 8b). Only $[C_4mim][PF_6]$ seems to show a deviation from Arrhenian behavior although the temperature range studied for the other ionic liquids is too narrow to conclude.

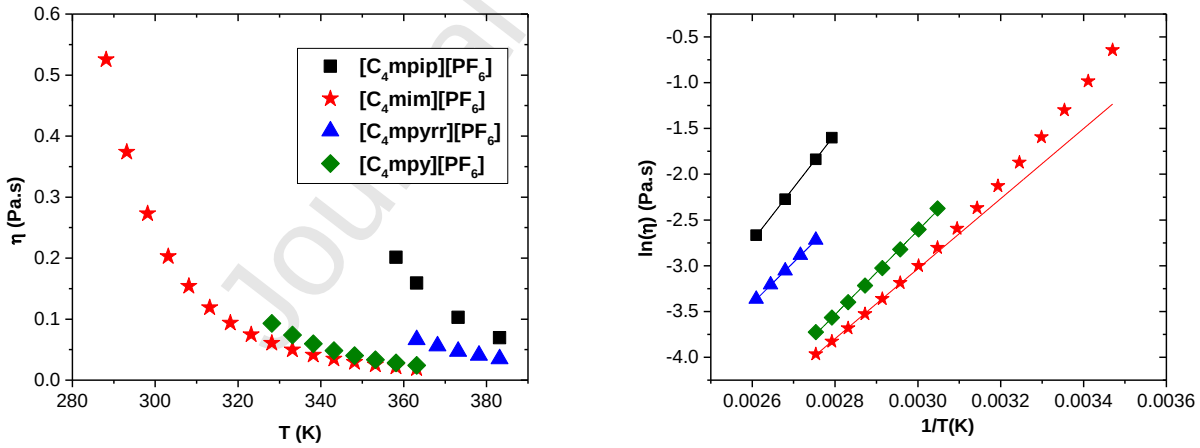

(a) (b)

Figure 8: (a) Viscosity of pure ionic liquids; (b) Corresponding Arrhenius plots (the lines are linear fits to ln η = f(1/T) in the high-temperature range).

The viscosity of all pure ionic liquids was fitted with equation (9) and the parameters along with the average absolute relative deviation (AARD) calculated using equation (16) are reported in Table 5. In addition, fits of the viscosity data over the entire temperature range for all pure ionic liquids with the Arrhenius equation (15) were performed and the corresponding AARD are reported in Table 5 as well.

$$AARD = \frac{1}{N}\sum_{i=1}^{N}\frac{|\eta_{calc}(T_i) - \eta_{exp}(T_i)|}{\eta_{exp}(T_i)}\ 100\ \% \qquad (16)$$

Table 5: Optimized MYEGA parameters for pure ionic liquids and deviations for MYEGA and Arrhenius equations

IL	B	C	AARD MYEGA (%)	AARD Arrhenius (%)
[C_4mpyrr][PF_6]	456	526	0.26	0.26
[C_4mpy][PF_6]	320	579	0.08	1.47
[C_4mpip][PF_6]	416	615	0.15	0.73
[C_4mim][PF_6]	370	506	0.26	11.90

For all pure ionic liquids, the MYEGA equation provided a better fit of the viscosity data than the Arrhenius-type equation using the same number of adjustable parameters.

4.2.2.2 Binary Mixtures

For the binary mixtures involving [C_4mpy][PF_6] (Figures 9a,b,e,f), the viscosity increases dramatically with the mole fraction of either [C_4mpip][PF_6] or [C_4mpyrr][PF_6]. This trend is even more pronounced at low temperatures. For the [C_4mpip][PF_6]-[C_4mpyrr][PF_6] system (Figures 9c and 9d), the viscosity increases in a similar fashion with the mole fraction of [C_4mpip][PF_6]. The viscosity of the binary mixtures is always lying between that of the two corresponding pure ionic liquids.

The viscosity of all binary mixtures was fitted with the model described in section 3.2. For the sake of clarity, results for only a few selected compositions and temperatures are presented here in Figure 9. The corresponding AARD, maximum absolute deviation in Pa.s (Max Δη) and its corresponding absolute relative deviation (Max ARD) along with the optimized k_{ij} binary parameters are reported in Table 6.

The performance of the developed viscosity model was compared with the Grunberg-Nissan [26] mixing law:

$$\ln \eta_{mix} = \sum_i x_i \ln \eta_i + \sum_{i \neq j} \sum_j x_i x_j G_{ij} \quad (17)$$

where η_i is the viscosity of the pure ionic liquid i, x_i represents its mole fraction in the mixture, and G_{ij} is an interaction parameter that can either be a constant or a function of temperature. In this work, G_{ij} was taken as independent of temperature in order to keep the same number of adjustable parameters and ensure a fair comparison between both approaches. The corresponding AARD, maximum absolute deviation in Pa.s (Max Δη) and its corresponding absolute relative deviation (Max ARD) along with the optimized G_{ij} binary parameters are reported in Table 7.

The proposed model provides a better fit of the viscosity data than the Grunberg-Nissan mixing law. The largest deviations for the latter were observed for the [C_4mpip][PF_6]-[C_4mpy][PF_6] binary system, for which the difference between the viscosities of the two corresponding pure compounds is the largest.

Table 6: Optimized binary parameters for the proposed model and corresponding deviations

	k_{ij}	AARD (%)	Max Δη (Pa.s)	Max ARD (%)
[C_4mpy][PF_6]-[C_4mpyrr][PF_6]	0.0192	1.94	0.021	2.83
[C_4mpip][PF_6]-[C_4mpyrr][PF_6]	-0.0024	2.47	0.004	2.77
[C_4mpip][PF_6]-[C_4mpy][PF_6]	0.0132	0.72	0.020	0.61
Total		1.71		

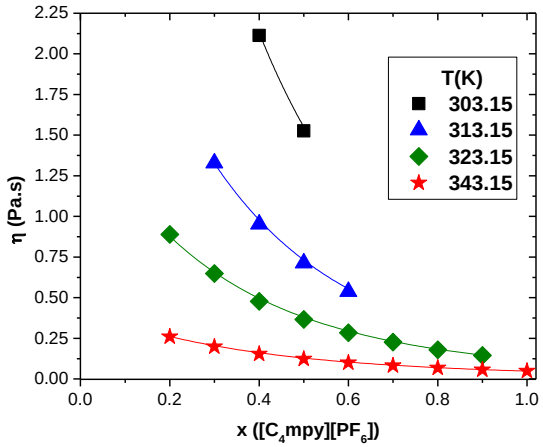

(a)

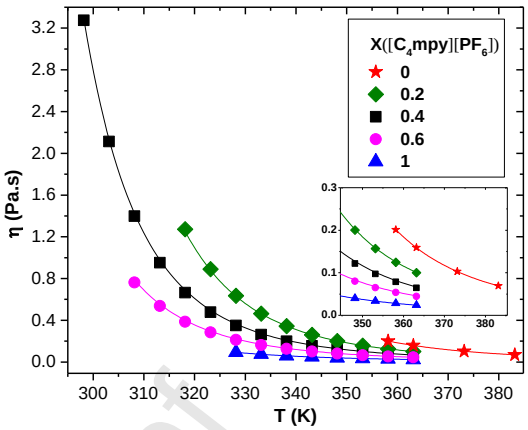

(b)

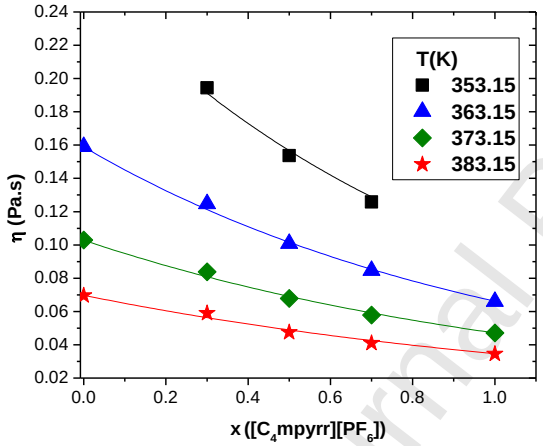

(c)

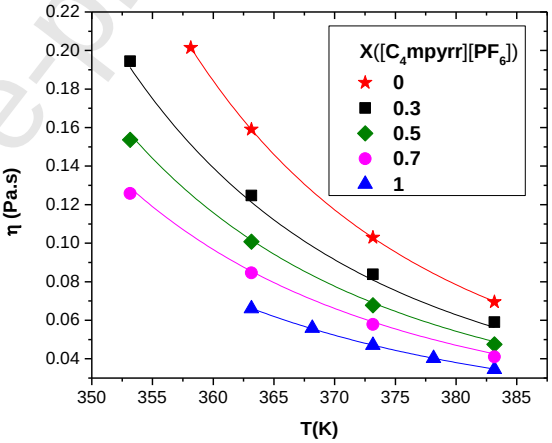

(d)

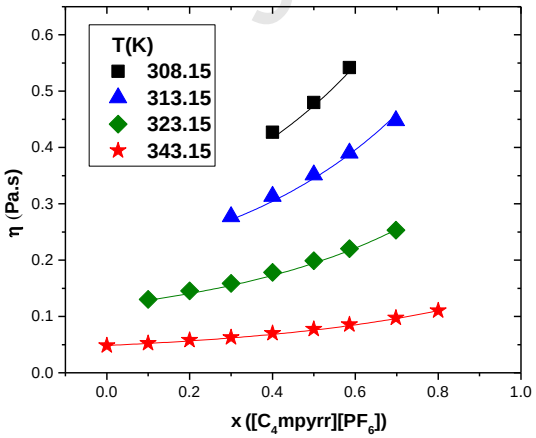

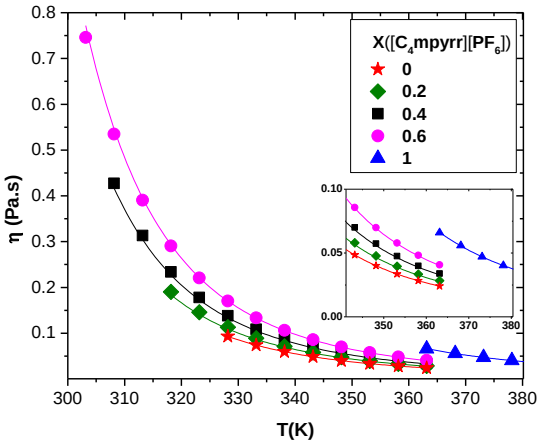

(e) (f)

Figure 9: Calculated (fitted) viscosity with the proposed model of the $[C_4mpip][PF_6]$-$[C_4mpy][PF_6]$ binary mixtures as a function of: (a) mole fraction of $[C_4mpy][PF_6]$ and (b) temperature; of the $[C_4mpip][PF_6]$-$[C_4mpyrr][PF_6]$ binary mixtures as a function of: (c) mole fraction of $[C_4mpyrr][PF_6]$ and (d) temperature; and of the $[C_4mpy][PF_6]$-$[C_4mpyrr][PF_6]$ binary mixtures as a function of: (e) mole fraction of $[C_4mpyrr][PF_6]$ and (f) temperature

Table 7: Optimized binary interaction parameters for the Grunberg-Nissan mixing law and corresponding deviations

	G_{ij}	AARD (%)	Max Δη (Pa.s)	Max ARD (%)
$[C_4mpy][PF_6]$-$[C_4mpyrr][PF_6]$	-0.6091	3.98	0.035	4.60
$[C_4mpip][PF_6]$-$[C_4mpyrr][PF_6]$	-0.0439	2.40	0.004	2.89
$[C_4mpip][PF_6]$-$[C_4mpy][PF_6]$	-1.1304	6.84	0.109	3.27
Total		4.36		

4.2.2.3 Ternary Mixtures

The predictive ability of the developed viscosity model was tested on the viscosity of the ternary mixtures investigated. No additional adjustable parameter was used. Good agreement between the experimental data and predicted viscosities was obtained as seen in Figures 10a,b and 11a,b. The corresponding AARD, Max Δη, and Max ARD are reported in Table 8.

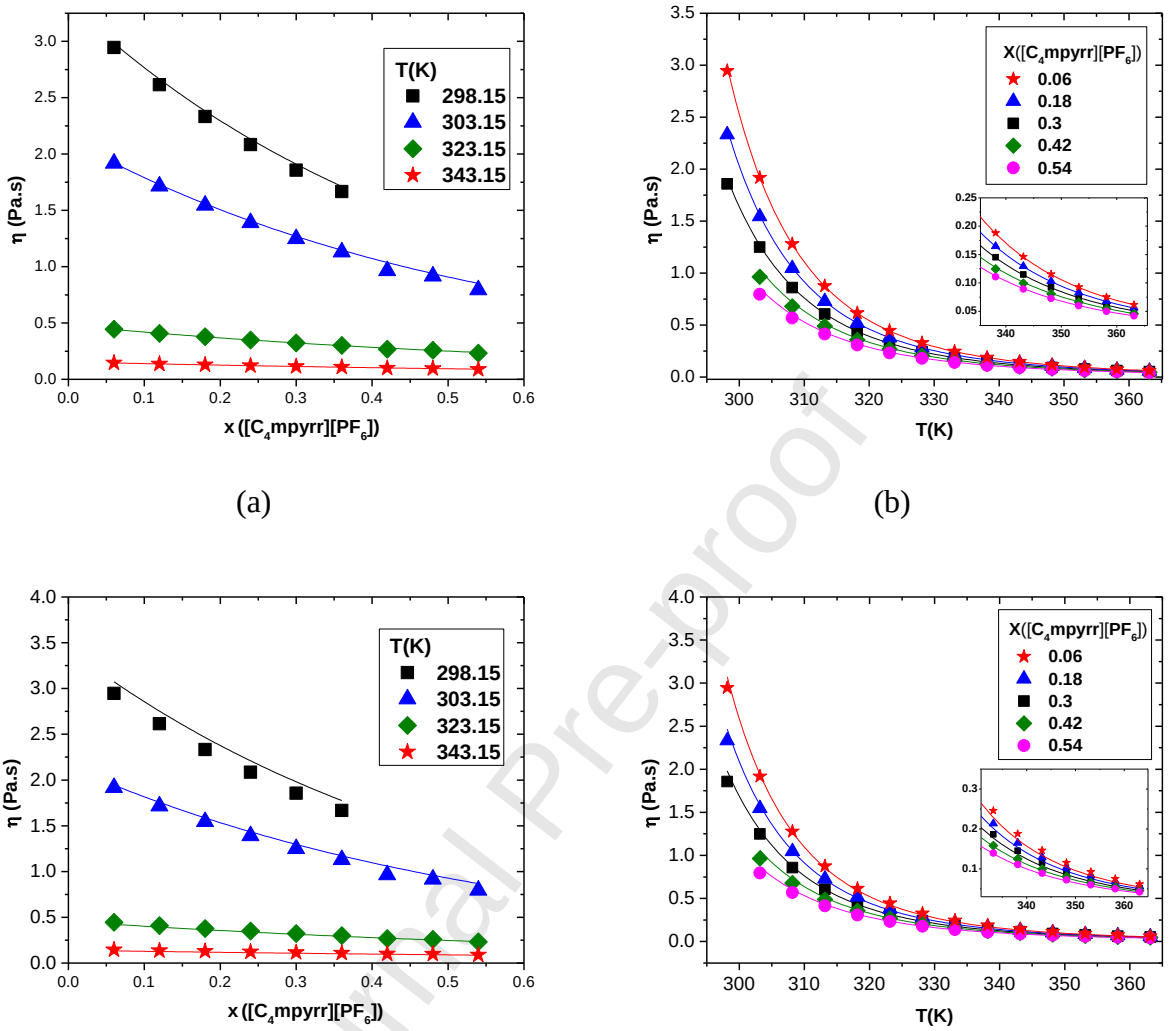

(a) (b)

(c) (d)

Figure 10: Calculated (predicted) viscosity of $[C_4mpy][PF_6]$(1)-$[C_4mpip][PF_6]$(2)-$[C_4mpyrr][PF_6]$(3) ternary mixtures at constant $x_1 = 0.4$ with the proposed model as a function of: (a) $[C_4mpyrr][PF_6]$ mole fraction and (b) temperature; and with the Grunberg-Nissan mixing law as a function of: (c) $[C_4mpyrr][PF_6]$ mole fraction and (d) temperature

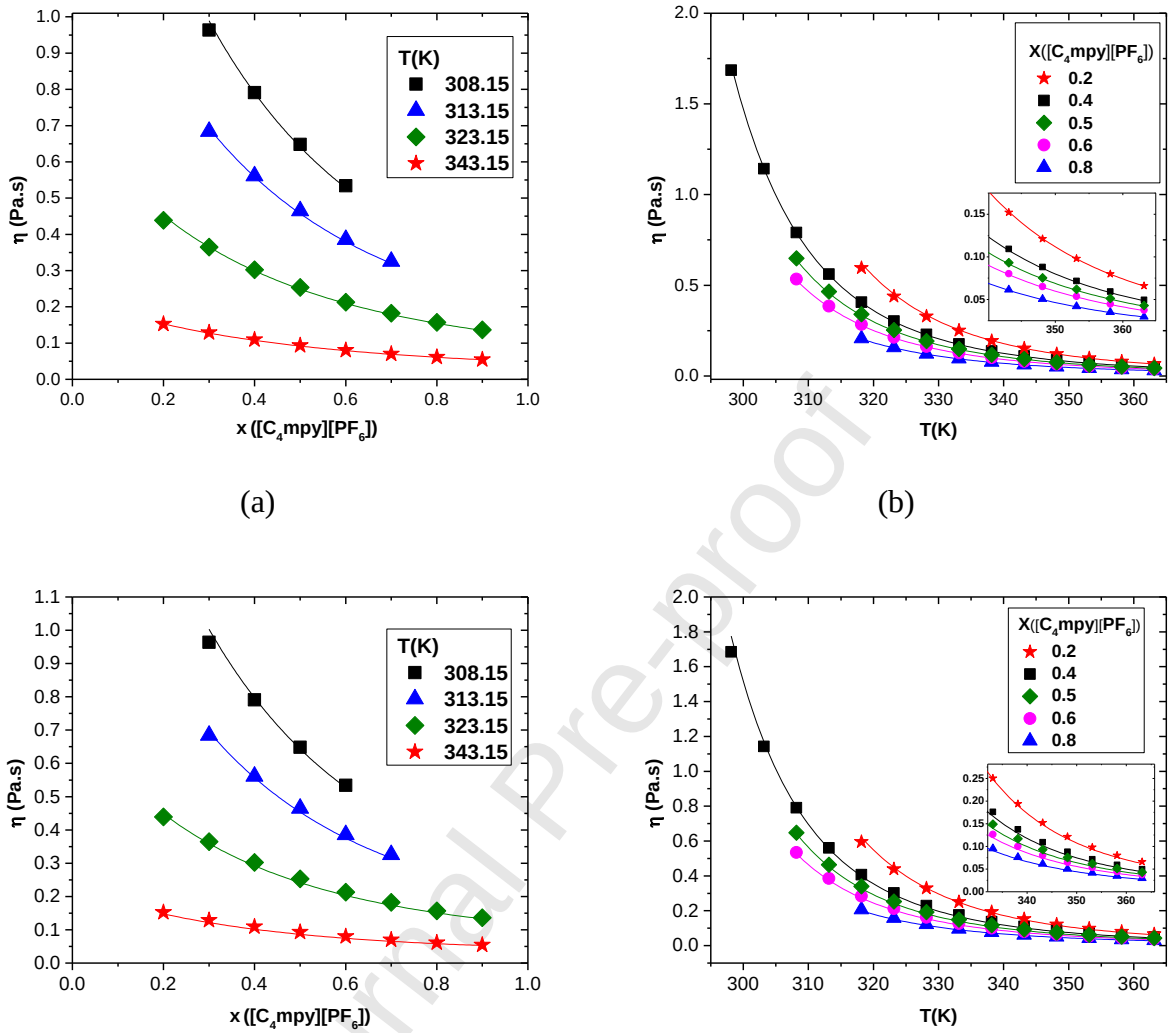

Figure 11: Calculated (predicted) viscosity of $[C_4mpy][PF_6]$(1)-$[C_4mpip][PF_6]$(2)-$[C_4mpyrr][PF_6]$(3) ternary mixtures at constant $x_3 / (x_2 + x_3) = 0.6$ with the proposed model as a function of: (a) $[C_4mpy][PF_6]$ mole fraction and (b) temperature; and with the Grunberg-Nissan mixing law as a function of: (c) $[C_4mpy][PF_6]$ mole fraction and (d) temperature

Table 8: Deviations of the proposed viscosity model for predicted ternary data

Isoplethal section	**AARD (%)**	**Max Δη (Pa.s)**	**Max ARD (%)**
$\boldsymbol{x_{[C_4mpy][PF_6]} = 0.4}$	1.22	0.075	7.73

$\frac{x_{[C_4mpyrr][PF_6]}}{x_{[C_4mpyrr][PF_6]} + x_{[C_4mpip][PF_6]}} = 0.6$	1.34	0.030	1.80
Total	1.28		

The results for the predictions of ternary data using equation (17) are displayed in Figures 10c,d and 11c,d. The predictive ability of the Grunberg-Nissan mixing law is somewhat poorer than that of the viscosity model proposed in this work. Deviations of up to 0.138 Pa.s are observed. The deviations for the Grunberg-Nissan mixing law are reported for ternary data in Table 9.

Table 9: Deviations of the Grunberg-Nissan mixing law for predicted ternary data

Isoplethal section	**AARD (%)**	**Max Δη (Pa.s)**	**Max ARD (%)**
$x_{[C_4mpy][PF_6]} = 0.4$	4.99	0.138	5.26
$\frac{x_{[C_4mpyrr][PF_6]}}{x_{[C_4mpyrr][PF_6]} + x_{[C_4mpip][PF_6]}} = 0.6$	4.85	0.090	5.35
Total	4.92		

Figure 12 shows that both approaches systematically overestimate the viscosity at low temperatures. Yet, the proposed model narrows the error range without any additional parameter.

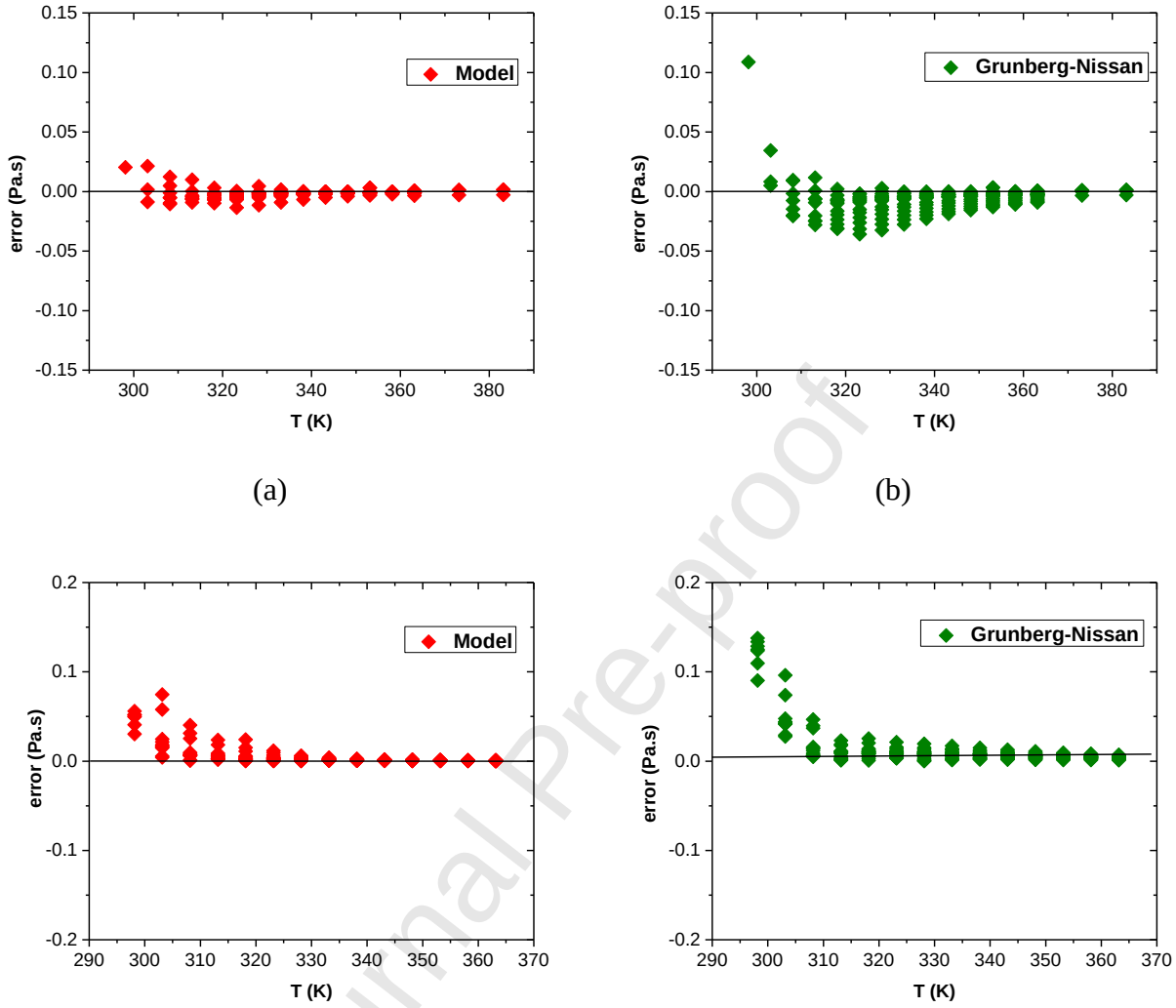

Figure 12: Absolute deviations between the fitted and the experimental unary and binary viscosities for (a) the proposed viscosity model and (b) the Grunberg-Nissan mixing law; and absolute deviations between the predicted and the experimental ternary viscosities for (c) the proposed viscosity model and (d) the Grunberg-Nissan mixing law

The purpose of the proposed viscosity model is to be able to assess the viscosity of ternary melts at any temperature and composition. In order to map the viscosity on the entire composition range at a desired operating temperature, one can plot iso-viscosity curves on the relevant isothermal section. This makes it possible to easily visualize the compositions of interest for a targeted viscosity at a given temperature. The predicted iso-viscosity curves at 318 and 363 K for

$[C_4mpyrr][PF_6]$-$[C_4mpy][PF_6]$-$[C_4mpip][PF_6]$ ternary melts over the entire composition range are shown in Figure 13. In each case, the iso-viscosity curves are only drawn in the region of composition where no solid phase precipitates.

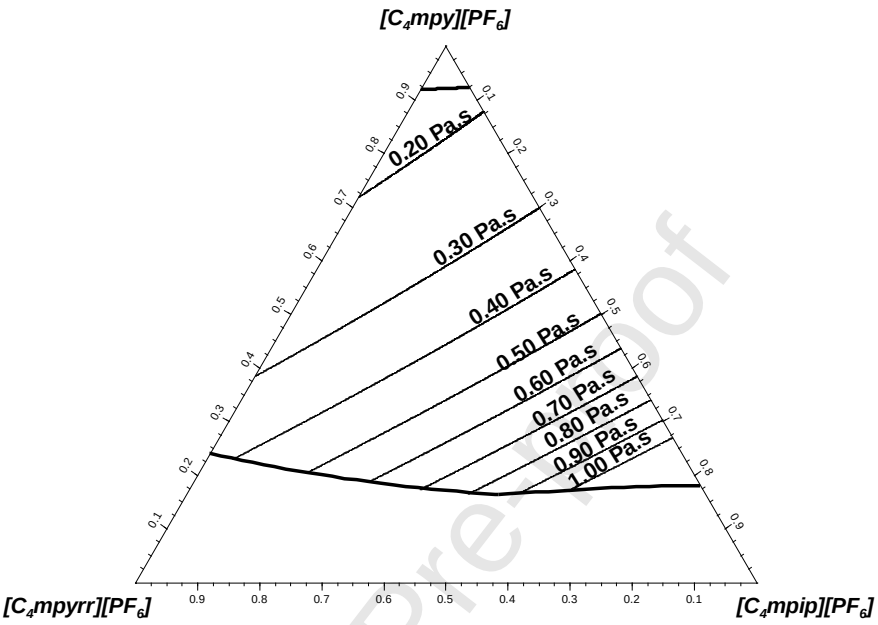

(a)

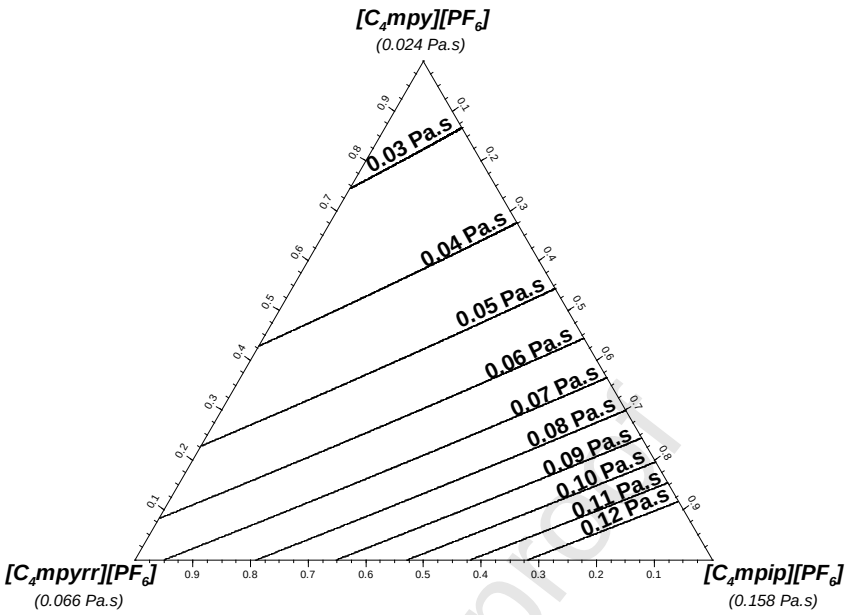

(b)

Figure 13: Predicted iso-viscosity curves with the proposed model for $[C_4mpy][PF_6]$-$[C_4mpyrr][PF_6]$-$[C_4mpip][PF_6]$ melts at: (a) 318 K and (b) 363 K

To the best of our knowledge, this is one of the first attempts to derive model parameters for the viscosity of binary mixtures of ionic liquids using data below the temperature of fusion of the pure components, with a minimum number of adjustable parameters. The error and the temperature seem to be correlated, which suggests that the problem stems from the temperature dependence used in the model.

Crespo *et al.* mentioned a similar issue while attempting to model the viscosity of Deep-Eutectic solvents using the Free Volume Theory [35]. These authors reported the inability of the three-parameter model to reproduce the viscosity over the entire temperature range and suggested to introduce additional parameters via the temperature dependence of the overlap parameter. However, to retain an economical model (three parameters for each pure component and 1 binary parameter), they simply reduced the temperature range considered and avoided fitting low-temperature viscosities which were not of interest for practical applications anyway.

However, the addition of adjustable parameters does not seem to correct this problem. In the work of Mjalli and Naser [38] describing a model adapted from Eyring's theory and the VFT equation and applied to the viscosity of choline chloride-based Deep-Eutectic solvents (DES), significant deviations were observed at low temperatures, even with 7 adjustable parameters derived for the binary mixture.

According to equation (8), the configurational entropy for a pure liquid has the following temperature dependence:

$$S_c(T) = A \exp\left(-\frac{B}{T}\right) \tag{18}$$

We attempted to fit the configurational entropy $S_c(T)$ of liquid [C_4mim][PF_6] derived by Ribeiro [58] from previous heat capacity measurements [73], using equation (18). The results are displayed in Figure 14.

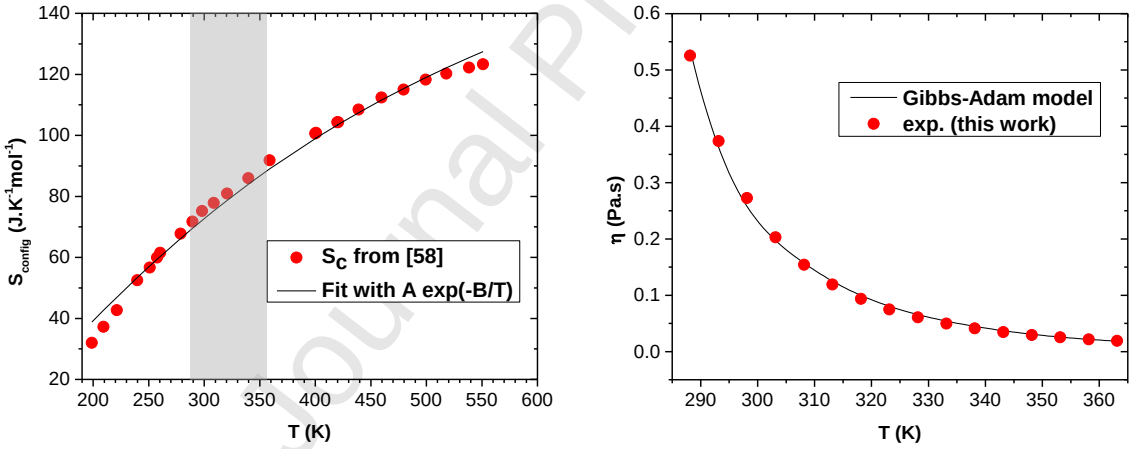

(a) (b)

Figure 14: (a) Fit of the configurational entropy of liquid [C_4mim][PF_6] [58] with equation (18). The highlighted area is the temperature range used for the fit of the viscosity of [C_4mim][PF_6]; (b) Fit using the Gibbs-Adam equation (7)

As can be seen in Figure 14, while the agreement seems acceptable in the temperature range of interest (highlighted), the extrapolation in the supercooled region leads in this case to an overestimation of $S_c(T)$, meaning that this expression for the configurational entropy, although simple, is not appropriate (at least for this type of ionic liquids) and may explain the observed discrepancies at low temperatures.

Considering the complex and diverse interactions in pure ionic liquids and their mixtures, it seems reasonable to assume a nontrivial dependence on the temperature and composition of the mixture's configurational entropy. This gives perspective for future work on the determination of the configurational entropy of ionic liquid mixtures to further understand the relationship between structure and dynamics in glass-forming ionic liquids.

5. Conclusions

In this work, new viscosity and density data for the [C_4mpyrr][PF_6], [C_4mpy][PF_6] and [C_4mpip][PF_6] ionic liquids and their binary and ternary mixtures were measured. Preliminary determination of the binary and ternary phase diagrams using DSC measurements and phase equilibria calculations with the FactSage thermochemical software [52] made it possible to measure the density/viscosity over the widest possible ranges of temperature and composition. The liquid solution was modelled using the Modified Quasichemical Model [54] and the solid solutions were described with the Compound Energy Formalism [55]. The used approach was similar to that in our previous work on a common-anion quaternary system consisting of the shorter-chain analogues of the ionic liquids studied in this work ([C_3mpyrr][PF_6], [C_3mpy][PF_6], [C_3mpip][PF_6] and [C_3mim][PF_6]) [49].

The mixing behavior of the C_4 ILs is akin to the C_3 analogues: the [C_4mpyrr][PF_6]-[C_4mpip][PF_6] system displays extensive solid solubility due to the similar cation structure of the pure components, whereas the two binary systems comprising [C_4mpy][PF_6] exhibit a simple eutectic behavior with negligible solid solubility. In all cases, the liquid phase behavior was close to ideal with small Gibbs energy of the pair-exchange reactions ($\Delta g_{AB/PF6} < 1$kJ/mol). The ternary phase diagram of the system [C_4mpyrr][PF_6]-[C_4mpy][PF_6]-[C_4mpip][PF_6] was calculated from the optimized binary parameters using an asymmetric interpolation method with [C_4mpy][PF_6] as the asymmetric component. No ternary excess parameter was introduced nor were the binary parameters adjusted to fit the ternary phase equilibria data. The agreement was overall satisfactory except for thermal transitions observed in the isoplethal section at constant 40 mol % [C_4mpy][PF_6] which were not accounted for by the thermodynamic model and, interestingly

enough, were also observed by Mirarabrazi *et al.* [49] for the C_3 analogues over the same composition range. Those were believed to correspond to metastable phase equilibria; the results in this work tend to support this hypothesis. Further investigation using structural studies is recommended for future work.

The viscosity data allowed to parametrize a new viscosity model for mixtures based on the MYEGA equation [46] and to test its predictive ability on ternary mixtures. The new model was compared to the Grunberg-Nissan mixing law using the same number of adjustable parameters. Both approaches tend to overestimate the viscosity at low temperatures with our model exhibiting somewhat smaller deviations (Max $\Delta\eta$ 0.075 vs 0.138 Pa.s). A fit of the configurational entropy of liquid $[C_4mim][PF_6]$ from Ribeiro [58] over a large temperature range suggests that the expression proposed by Mauro *et al*. [46] may not be appropriate for this type of liquids, which would explain the discrepancy observed. Nevertheless, the proposed approach gives satisfactory results, especially for predictions in ternary mixtures (AARD of 1.28 %) with a simple expression for the configurational entropy and few adjustable binary parameters.

As a fair number of common-ion ionic liquid mixtures show little deviation from ideality, one could estimate the pair fractions from the mole fractions, thus adding to the simplicity of the model. However, this approximation would be insufficient in the case of non-ideal liquid mixtures and is incorrect for ternary reciprocal mixtures (i.e. with two different anions and two different cations: [A][X]-[B][Y]) for which quadruplet fractions must be used. The application of the proposed model to such mixtures would test its ability to capture the composition dependence of viscosity in the case of substantial deviations from ideality.

Conflicts of interest

There are no conflicts to declare.

Acknowledgements

This work was developed within the scope of the project CICECO-Aveiro Institute of Materials, UIDB/50011/2020 & UIDP/50011/2020, financed by national funds through the FCT/MEC and

when appropriate co-financed by FEDER under the PT2020 Partnership Agreement. The modeling part of this project was supported by the Natural Sciences and Engineering Research Council of Canada (Discovery Grant RGPIN 435893-2013). Anya F. Bouarab acknowledges a MITACS Globalink Research Award for her 12-week experimental internship at CICECO-Aveiro Institute of Materials. Olga Stolarska is grateful to the European Union for the support via grant no. POWR.03.02.00-00-I023/17 co-financed by the European Union through the European Social Fund under the Operational Program Knowledge Education Development. Marcin Smiglak acknowledges financial support from the National Science Centre (Poland), project SONATA (No. 2011/03/D/ST5/06200).

References

[1] M. J. Earle and K. R. Seddon, "Ionic liquids: Green solvents for the future", *Pure and applied chemistry*, vol. 72, no. 7, pp. 1391-1398, 2000.

[2] K. R. Seddon, "Ionic liquids: Designer solvents ?", in *The International George Papatheodorou Symposium: Proceedings*, 1999, pp. 131-135, Institute of Chemical Engineering and High Temperature Chemical Processes, Patras, Greece.

[3] J. J. H. Davis, "Task-specific ionic liquids", *Chem. Lett.*, vol. 33, no. 9, pp. 1072-1077, 2004.

[4] N. V. Plechkova and K. R. Seddon, "Applications of ionic liquids in the chemical industry", *Chem. Soc. Rev.*, vol. 37, no. 1, pp. 123-50, Jan 2008.

[5] A. S. Ivanova, T. Brinzer, E. A. Roth, V. A. Kusuma, J. D. Watkins, X. Zhou, D. Luebke, D. Hopkinson, N. R. Washburn, S. Garrett-Roe, and H. B. Nulwala, "Eutectic ionic liquid mixtures and their effect on co2 solubility and conductivity", *RSC Advances*, vol. 5, no. 63, pp. 51407-51412, 2015.

[6] M. Kunze, S. Jeong, G. B. Appetecchi, M. Schönhoff, M. Winter, and S. Passerini, "Mixtures of ionic liquids for low temperature electrolytes", *Electrochimica Acta*, vol. 82, pp. 69-74, 2012.

[7] E. P. Yambou, B. Gorska, and F. Béguin, "Binary mixtures of ionic liquids based on emim cation and fluorinated anions: Physico-chemical characterization in view of their application as low-temperature electrolytes", *Journal of Molecular Liquids*, p. 111959, 2019/10/21/ 2019.

[8] L. Timperman, A. Vigeant, and M. Anouti, "Eutectic mixture of protic ionic liquids as an electrolyte for activated carbon-based supercapacitors", *Electrochimica Acta*, vol. 155, pp. 164-173, 2015/02/10/ 2015.

[9] R. Newell, J. Faure-Vincent, B. Iliev, T. Schubert, and D. Aradilla, "A new high performance ionic liquid mixture electrolyte for large temperature range supercapacitor

applications (−70 °c to 80 °c) operating at 3.5v cell voltage", *Electrochimica Acta*, vol. 267, pp. 15-19, 2018/03/20/ 2018.

[10] M. Taige, D. Hilbert, and T. J. S. Schubert, "Mixtures of ionic liquids as possible electrolytes for lithium ion batteries", *Zeitschrift für Physikalische Chemie*, vol. 226, no. 2, pp. 129-139, 2012.

[11] T. Vogl, S. Passerini, and A. Balducci, "The impact of mixtures of protic ionic liquids on the operative temperature range of use of battery systems", *Electrochemistry Communications*, vol. 78, pp. 47-50, 2017/05/01/ 2017.

[12] P. M. Bayley, A. S. Best, D. R. MacFarlane, and M. Forsyth, "Transport properties and phase behaviour in binary and ternary ionic liquid electrolyte systems of interest in lithium batteries", *ChemPhysChem*, vol. 12, no. 4, pp. 823-827, 2011.

[13] Y. Bai, Y. Cao, J. Zhang, M. Wang, R. Li, P. Wang, S. M. Zakeeruddin, and M. Grätzel, "High-performance dye-sensitized solar cells based on solvent-free electrolytes produced from eutectic melts", *Nature Materials*, vol. 7, no. 8, pp. 626-630, 2008/08/01 2008.

[14] Y. Cao, J. Zhang, Y. Bai, R. Li, S. M. Zakeeruddin, M. Grätzel, and P. Wang, "Dye-sensitized solar cells with solvent-free ionic liquid electrolytes", *The Journal of Physical Chemistry C*, vol. 112, no. 35, pp. 13775-13781, 2008/09/04 2008.

[15] O. Stolarska, A. Pawlowska-Zygarowicz, A. Soto, H. Rodriguez, and M. Smiglak, "Mixtures of ionic liquids as more efficient media for cellulose dissolution", *Carbohyadr. Polym.*, vol. 178, pp. 277-285, 2017.

[16] A. M. Pinto, H. Rodríguez, Y. J. Colón, A. Arce, A. Arce Jr., and A. Soto, "Absorption of carbon dioxide in two binary mixtures of ionic liquids", *Industrial & Engineering Chemistry Research*, vol. 52, no. 17, pp. 5975-5984, 2013/05/01 2013.

[17] A. Finotello, J. E. Bara, S. Narayan, D. Camper, and R. D. Noble, "Ideal gas solubilities and solubility selectivities in a binary mixture of room-temperature ionic liquids", *The Journal of Physical Chemistry B*, vol. 112, no. 8, pp. 2335-2339, 2008/02/01 2008.

[18] L. C. Tomé, D. J. S. Patinha, C. S. R. Freire, L. P. N. Rebelo, and I. M. Marrucho, "Co2 separation applying ionic liquid mixtures: The effect of mixing different anions on gas permeation through supported ionic liquid membranes", *RSC Advances*, vol. 3, no. 30, pp. 12220-12229, 2013.

[19] D. Azizi and F. Larachi, "Immiscible dual ionic liquid-ionic liquid mineral separation of rare-earth minerals", *Separation and Purification Technology*, vol. 191, pp. 340-353, 2018.

[20] F. Llovell and L. F. Vega, "Assessing ionic liquids experimental data using molecular modeling: [cnmim][bf4] case study", *Journal of Chemical & Engineering Data*, vol. 59, no. 10, pp. 3220-3231, 2014/10/09 2014.

[21] Y. Sun, G. Shen, C. Held, X. Lu, and X. Ji, "Modeling viscosity of ionic liquids with electrolyte perturbed-chain statistical associating fluid theory and free volume theory", *Industrial & Engineering Chemistry Research*, vol. 57, p. 8784−8801, 2018/06/04 2018.

[22] S. M. Hosseini, M. M. Alavianmehr, and J. Moghadasi, "Transport properties of pure and mixture of ionic liquids from new rough hard-sphere-based model", *Fluid Phase Equilibria*, vol. 429, pp. 266-274, 2016.

[23] S. Atashrouz, M. Zarghampour, S. Abdolrahimi, G. Pazuki, and B. Nasernejad, "Estimation of the viscosity of ionic liquids containing binary mixtures based on the eyring's theory and a modified gibbs energy model", (in English), *J. Chem. Eng. Data*, vol. 59, no. 11, pp. 3691-3704, 2014.

[24] N. Zhao, J. Jacquemin, R. Oozeerally, and V. Degirmenci, "New method for the estimation of viscosity of pure and mixtures of ionic liquids based on the unifac-visco model", *Journal of Chemical & Engineering Data,* vol. 61, no. 6, pp. 2160-2169, 2016.

[25] J. O. Valderrama, L. F. Cardona, and R. E. Rojas, "Correlation of ionic liquid viscosity using valderrama-patel-teja cubic equation of state and the geometric similitude concept. Part ii: Binary mixtures of ionic liquids", *Fluid Phase Equilibria,* vol. 497, pp. 178-194, 2019/05/03/ 2019.

[26] L. Grunberg and A. H. Nissan, "Mixture law for viscosity", *Nature,* vol. 164, no. 4175, pp. 799-800, 1949.

[27] P. K. Katti and M. M. Chaudhri, "Viscosities of binary mixtures of benzyl acetate with dioxane, aniline, and m-cresol", *Journal of Chemical & Engineering Data,* vol. 9, no. 3, pp. 442-443, 1964/07/01 1964.

[28] H. Niedermeyer, J. P. Hallett, I. J. Villar-Garcia, P. A. Hunt, and T. Welton, "Mixtures of ionic liquids", *Chem. Soc. Rev.,* vol. 41, no. 23, pp. 7780-802, Dec 7 2012.

[29] N. S. M. Vieira, I. Vázquez-Fernández, J. M. M. Araújo, N. V. Plechkova, K. R. Seddon, L. P. N. Rebelo, and A. B. Pereiro, "Physicochemical characterization of ionic liquid binary mixtures containing 1-butyl-3-methylimidazolium as the common cation", *Journal of Chemical & Engineering Data,* vol. 64, pp. 4891-4903, 2019/10/04 2019, Art. no. J. Chem. Eng. Data.

[30] H. Vogel, "The law of the relation between the viscosity of liquids and the temperature", *Physikalische Zeitschrift,* vol. 22, p. 645, 1921.

[31] G. S. Fulcher, "Analysis of recent measurements of the viscosity of glasses. Ii", *Journal of the American Ceramic Society,* vol. 8, no. 12, pp. 789-794, 1925.

[32] G. Tammann and W. Hesse, "Die abhängigkeit der viscosität von der temperatur bie unterkühlten flüssigkeiten", *Zeitschrift für anorganische und allgemeine Chemie,* vol. 156, no. 1, pp. 245-257, 1926.

[33] F. Castiglione, G. Raos, G. Battista Appetecchi, M. Montanino, S. Passerini, M. Moreno, A. Famulari, and A. Mele, "Blending ionic liquids: How physico-chemical properties change", *Physical Chemistry Chemical Physics,* vol. 12, no. 8, pp. 1784-1792, 2010.

[34] C. A. Angell, "Structural instability and relaxation in liquid and glassy phases near the fragile liquid limit", *Journal of Non-Crystalline Solids,* vol. 102, no. 1, pp. 205-221, 1988/06/01/ 1988.

[35] E. A. Crespo, J. M. L. Costa, A. M. Palma, B. Soares, M. C. Martín, J. J. Segovia, P. J. Carvalho, and J. A. P. Coutinho, "Thermodynamic characterization of deep eutectic solvents at high pressures", *Fluid Phase Equilibria,* vol. 500, p. 112249, 2019/11/15/ 2019.

[36] J. Gross and G. Sadowski, "Perturbed-chain saft: An equation of state based on a perturbation theory for chain molecules", *Industrial & Engineering Chemistry Research,* vol. 40, no. 4, pp. 1244-1260, 2001/02/01 2001.

[37] R. Haghbakhsh, K. Parvaneh, S. Raeissi, and A. Shariati, "A general viscosity model for deep eutectic solvents: The free volume theory coupled with association equations of state", *Fluid Phase Equilibria,* vol. 470, pp. 193-202, 2018/08/25/ 2018.

[38] F. S. Mjalli and J. Naser, "Viscosity model for choline chloride-based deep eutectic solvents", *Asia-Pacific Journal of Chemical Engineering,* vol. 10, no. 2, pp. 273-281, 2015.

[39] C. Alba-Simionesco, "Salient properties of glassforming liquids close to the glass transition", *Comptes Rendus de l'Académie des Sciences - Series IV - Physics-Astrophysics,* vol. 2, no. 2, pp. 203-216, 2001/03/01/ 2001.

[40] G. Tarjus, D. Kivelson, S. Mossa, and C. Alba-Simionesco, "Disentangling density and temperature effects in the viscous slowing down of glassforming liquids", *The Journal of Chemical Physics,* vol. 120, no. 13, pp. 6135-6141, 2004.

[41] N. Kaoru, K. Naoki, and T. Noriyuki, "Non-aqueous electrolyte solution and lithium-ion secondary battery", WO Patent 2018096889A1, 2018. Available: https://patents.google.com/patent/WO2018096889A1/en.

[42] C. Siret, P. Biensan, and L. Caratero, "Lithium-ion battery containing an electrolyte comprising an ionic liquid", US Patent 9543617B2, 2017. Available: https://patents.google.com/patent/US9543617B2/en.

[43] P. Verma, M. Donotek, S. Hahn, T. Schonhardt, and E. Buehler, "Hybrid supercapacitor", US Patent 20170069434, 2017. Available: https://patents.google.com/patent/US20170069434A1/en.

[44] J. F. Denatale and M. W. Kendig, "Microfabricated liquid junction reference electrode", US Patent 8211283B2, 2012. Available: https://patents.google.com/patent/US8211283B2/en.

[45] N. F. Atta, A. H. Ibrahim, and A. Galal, "Nickel oxide nanoparticles/ionic liquid crystal modified carbon composite electrode for determination of neurotransmitters and paracetamol", *New Journal of Chemistry,* vol. 40, no. 1, pp. 662-673, 2016.

[46] J. C. Mauro, Y. Yuanzheng, A. J. Ellison, P. K. Gupta, and D. C. Allan, "Viscosity of glass-forming liquids", *Proceedings of the National Academy of Sciences of the United States of America,* vol. 106, no. 47, pp. 19780-19784, 11/24 2009.

[47] L. Kaufman, *Computer calculation of phase diagrams with special reference to refractory metals* (no. Book, Whole). United States, 1970.

[48] A. Kroupa, "Modelling of phase diagrams and thermodynamic properties using calphad method – development of thermodynamic databases", *Computational Materials Science,* vol. 66, pp. 3-13, 2013/01/01/ 2013.

[49] M. Mirarabrazi, M. A. R. Martins, S. P. Pinho, J. A. P. Coutinho, and C. Robelin, "Solid–liquid equilibria for hexafluorophosphate-based ionic liquid quaternary mixtures and their corresponding subsystems", *The Journal of Physical Chemistry B,* vol. 123, no. 42, pp. 8954-8969, 2019/10/24 2019.

[50] M. Mirarabrazi, O. Stolarska, M. Smiglak, and C. Robelin, "Solid-liquid equilibria for a pyrrolidinium-based common-cation ternary ionic liquid system, and for a pyridinium-based ternary reciprocal ionic liquid system: An experimental study and a thermodynamic model", *Physical Chemistry Chemical Physics,* vol. 20, no. 1, pp. 637-657, 2018.

[51] L. Fernandez, L. P. Silva, M. A. R. Martins, O. Ferreira, J. Ortega, S. P. Pinho, and J. A. P. Coutinho, "Indirect assessment of the fusion properties of choline chloride from solid-liquid equilibria data", *Fluid Phase Equilibria,* vol. 448, pp. 9-14, 2017/09/25/ 2017.

[52] C. W. Bale, E. Bélisle, P. Chartrand, S. A. Decterov, G. Eriksson, A. E. Gheribi, K. Hack, I. H. Jung, Y. B. Kang, J. Melançon, A. D. Pelton, S. Petersen, C. Robelin, J. Sangster, P. Spencer, and M. A. Van Ende, "Factsage thermochemical software and databases, 2010–2016", *Calphad,* vol. 54, pp. 35-53, 2016/09/01/ 2016.

[53] P. Virtanen *et al.*, "Scipy 1.0-fundamental algorithms for scientific computing in python", *ArXiv*, vol. abs/1907.10121, 2019.
[54] A. D. Pelton, P. Chartrand, and G. Eriksson, "The modified quasi-chemical model: Part iv. Two-sublattice quadruplet approximation", *Metallurgical and Materials Transactions A*, vol. 32, no. 6, pp. 1409-1416, June 01 2001.
[55] M. Hillert, "The compound energy formalism", *Journal of Alloys and Compounds*, vol. 320, no. 2, pp. 161-176, 2001.
[56] G. Adam and J. H. Gibbs, "On the temperature dependence of cooperative relaxation properties in glass- forming liquids", *The Journal of Chemical Physics*, vol. 43, no. 1, pp. 139-146, 1965.
[57] O. Yamamuro, Y. Minamimoto, Y. Inamura, S. Hayashi, and H. Hamaguchi, "Heat capacity and glass transition of an ionic liquid 1-butyl-3-methylimidazolium chloride", *Chemical Physics Letters*, vol. 423, no. 4, pp. 371-375, 2006/06/01/ 2006.
[58] M. C. C. Ribeiro, "Correlation between quasielastic raman scattering and configurational entropy in an ionic liquid", *The Journal of Physical Chemistry B*, vol. 111, no. 18, pp. 5008-5015, 2007/05/01 2007.
[59] M. L. Williams, R. F. Landel, and J. D. Ferry, "The temperature dependence of relaxation mechanisms in amorphous polymers and other glass-forming liquids", *Journal of the American Chemical society*, vol. 77, no. 14, pp. 3701-3707, 1955.
[60] S. Waterton, "The viscosity-temperature relationship and some inferences on the nature of molten and of plastic glass", *J. Soc. Glass Technol.*, vol. 16, pp. 244-247, 1932.
[61] H. Le Chatelier, "Sur la viscosité du verre", *C. R. Acad. Sc. Paris*, vol. 179, pp. 517-21, 1924.
[62] G. G. Naumis, "Glass transition phenomenology and flexibility: An approach using the energy landscape formalism", *Journal of Non-Crystalline Solids*, vol. 352, no. 42, pp. 4865-4870, 2006/11/15/ 2006.
[63] Q. Zheng and J. C. Mauro, "Viscosity of glass- forming systems", *Journal of the American Ceramic Society*, vol. 100, no. 1, pp. 6-25, 2017.
[64] F. M. Gacino, T. Regueira, L. Lugo, M. J. P. Comunas, and J. Fernandez, "Influence of molecular structure on densities and viscosities of several ionic liquids", *Journal of Chemical & Engineering Data*, vol. 56, no. 12, pp. 4984-4999, 2011.
[65] G. J. Maximo, R. J. B. N. Santos, P. Brandão, J. M. S. S. Esperança, M. C. Costa, A. J. A. Meirelles, M. G. Freire, and J. A. P. Coutinho, "Generating ionic liquids from ionic solids: An investigation of the melting behavior of binary mixtures of ionic liquids", *Crystal Growth & Design*, vol. 14, no. 9, pp. 4270-4277, 2014/09/03 2014.
[66] J. Golding, N. Hamid, D. R. MacFarlane, M. Forsyth, C. Forsyth, C. Collins, and J. Huang, "N-methyl-n-alkylpyrrolidinium hexafluorophosphate salts: Novel molten salts and plastic crystal phases", *Chemistry of Materials*, vol. 13, no. 2, pp. 558-564, 2001/02/01 2001.
[67] M. Mirarabrazi, "Modeling the phase diagram and density of binary and ternary systems of ionic liquids", Maîtrise Mémoire de Maîtrise, Génie Chimique, Université de Montréal, École Polytechnique 2017.
[68] A. D. Pelton and P. Chartrand, "The modified quasi-chemical model: Part ii. Multicomponent solutions", *Metallurgical and Materials Transactions A*, journal article vol. 32, no. 6, pp. 1355-1360, June 01 2001.

[69] A. Bhattacharjee, P. J. Carvalho, and J. A. P. Coutinho, "The effect of the cation aromaticity upon the thermophysical properties of piperidinium- and pyridinium-based ionic liquids", *Fluid Phase Equilibria*, vol. 375, pp. 80-88, 2014/08/15/ 2014.

[70] M. Ribeiro, "Low-frequency raman spectra and fragility of imidazolium ionic liquids", *Journal of Chemical Physics*, vol. 133, no. 2, p. 024503, 2010.

[71] R. Tao, E. Gurung, M. M. Cetin, M. F. Mayer, E. L. Quitevis, and S. L. Simon, "Fragility of ionic liquids measured by flash differential scanning calorimetry", *Thermochimica Acta*, vol. 654, pp. 121-129, 2017/08/10/ 2017.

[72] W. Xu, E. I. Cooper, and C. A. Angell, "Ionic liquids: Ion mobilities, glass temperatures, and fragilities", *The Journal of Physical Chemistry B*, vol. 107, no. 25, pp. 6170-6178, 2003/06/01 2003.

[73] G. J. Kabo, A. V. Blokhin, Y. U. Paulechka, A. G. Kabo, M. P. Shymanovich, and J. W. Magee, "Thermodynamic properties of 1-butyl-3-methylimidazolium hexafluorophosphate in the condensed state", *Journal of Chemical & Engineering Data*, vol. 49, no. 3, pp. 453-461, 2004/05/01 2004.

CRediT author statement :

Anya F. Bouarab : Conceptualization, Methodology, Investigation, Writing - Original Draft, Writing - Review & Editing

Mónia A. R. Martins : Conceptualization, Methodology, Investigation, Writing - Review & Editing, Supervision

Olga Stolarska : Conceptualization, Methodology, Investigation, Writing - Review & Editing

Marcin Smiglak : Conceptualization, Methodology, Investigation, Writing - Review & Editing, Supervision, Funding acquisition

Jean-Philippe Harvey : Conceptualization, Methodology, Investigation, Writing - Review & Editing, Supervision

João A. P. Coutinho : Conceptualization, Methodology, Investigation, Writing - Review & Editing, Supervision, Funding acquisition

Christian Robelin : Conceptualization, Methodology, Investigation, Writing - Review & Editing, Supervision, Funding acquisition

Declaration of interests :

The authors declare that they have no known competing financial interests or personal relationships that could have appeared to influence the work reported in this paper.

HIGHLIGHTS :

- Phase diagram and viscosity measurements for a [PF_6]-based ternary IL system.

- Liquid thermodynamic model based on the Modified Quasichemical Model (MQM).

- The solid solutions were modeled with the Compound Energy Formalism (CEF).

- Viscosity model based on the Gibbs-Adam theory and the MQM.